2010

Qualitative and Quantitative X-Ray Diffraction Analysis for Forensic Examination of Duct Tapes

Rebecca E. Bucht
The Graduate Center, City University of New York

Qualitative and Quantitative X-Ray Diffraction Analysis for Forensic Examination of Duct Tapes

by

REBECCA E. BUCHT

A dissertation submitted to the Graduate Faculty in Criminal Justice in partial fulfillment of the requirements for the degree of Doctor of Philosophy,

The City University of New York

2010

This manuscript has been read and accepted for the

Graduate Faculty in Criminal Justice in satisfaction of the

dissertation requirement for the degree of Doctor of Philosophy.

	Dr. T.A. Kubic
_____	_____
Date	**Chair of Examining Committee**
	Dr. K. Terry
_____	_____
Date	**Executive Officer**

Dr. J. A. Reffner_____

Dr. N.D.K. Petraco_____

Supervisory Committee

THE CITY UNIVERSITY OF NEW YORK

Abstract

Qualitative and Quantitative X-Ray Diffraction Analysis

for Forensic Examination of Duct Tapes

by

Rebecca E. Bucht

Adviser: Dr. T.A. Kubic

Duct tapes are an increasingly important class of forensic evidence. This research has studied the value of using x-ray diffraction (XRD) to extend the ability of evidence examiners to gain additional information about a duct tape specimen.

Duct tapes are composed of five different layers. Starting from the non-adhesive side, these layers are the release coating, backing, scrim, primer and adhesive. The release coating assists in reducing unwind tension and preventing the tape from sticking to itself when on a roll. The backing layer serves as a support for the adhesive, and is usually based on polyethylene. The scrim is a layer of fibers either embedded in the backing layer or between the backing and adhesive layers. Primers help attach the adhesive to the backing. Pressure sensitive adhesives are based on polymers such as natural or synthetic rubbers combined with tackifying resins and hydrogenated resins. Pigments and additives are added to the backing and adhesive layers in order to achieve the desired tape characteristics and appearance.

A variety of instrumental methods are used to obtain information for discrimination of pressure sensitive tapes including duct tapes. Research has been reported on the evidential value of a range of physical investigations such as, physical and optical examination of thickness, weight/area, fluorescence, and birefringence, as well as instrumental chemical techniques including UV/VIS, FTIR, XRF, NAA, ICP MS, XRD, pyrolysis-GC/MS and isotope-ratio MS. XRD analyses have been used to identify minerals in duct tape but to date, only limited qualitative XRD information has been used and no systematic investigation of the further uses of XRD analysis and databases has been published.

XRD analysis has the potential to offer a convenient, cost effective and non-destructive method for further characterization of the molecular or atomic make up of the tape layers. The diffractogram contains information about the qualitative and quantitative mineral composition and the crystallinity of mineral species and polymers present.

This research has shown that the use of quantitative XRD analysis of duct tapes can differentiate between some duct tape samples from rolls that cannot be distinguished by current, routine analysis methods.

Acknowledgements:

I would like to acknowledge the Finnish Academy (Suomen Akatemia) for providing financial support and John Jay College of Criminal Justice for providing equipment and facilities for this research.

During my years at the Graduate Center and John Jay College, I have certainly been hoisted up on the proverbial shoulders of giants….

> I would like to thank my committee, Dr Kubic, Dr Reffner and Dr Petraco for their guidance and advice, not only with this dissertation but during all of my time at John Jay College. I would also like to express my gratitude to Dr De Forest for his mentorship and numerous contributions to my professional development.

…and I surely would not have managed to keep from tumbling down from those shoulders without some considerable help:

> I owe a great deal to Christina Czechowitz for all her moral support and advice. I also owe my thanks (and a few rounds of drinks) to my friends and family, both in NYC and abroad, for their encouragement and for always making sure I had a place (or several places) to call home.

Finally, it is with immense gratitude and love that I dedicate this dissertation to my parents, Stina and Harri Bucht.

Table of Contents

I. Context of this Study 1

Forensic science in and beyond the courtroom 1

Crime and the use of duct tape 3

II. Statement of the Problem and Literature Review 4

Duct tape composition 4

Manufacturing process 5

Polyethylene orientation and crystallinity 6

Mineral composition and quantity 7

Existing methodologies and technology for analysis 8

Statement of some current analytical problems 9

X-Ray diffraction 10

XRD in forensics 14

III. Approach and Methodology 16

Introduction 16

Research protocol 16

Samples 18

Qualitative comparison 19

Quantitative Comparison 19

Data pretreatment 20

PCA 21

CVA 22

LDA 24

Hold –one-Out verification 25

IV. Findings 26

Qualitative Comparisons: Results 26

Quantitative Comparisons: Results 27

Limitations of sample size 49

Polyethylene backing 51

Orientation Effects 53

Blind Validation Study 54

V. General Conclusions 74

Summary of results and recommended analysis scheme 74

Implications for policy and practice 75

Future Research 76

VII. Appendices 78

Appendix A Sample Information 78

Appendix B Within-roll Variation & Outliers 84

Appendix C Peaks used for Quantitative Comparisons 100

VII. Cited References 102

Table of Figures:

Figure 1: Diffraction of X-Rays in a lattice 11

Figure 2: Schematic of a 4-circle single-crystal diffractometer..... 13

Figure 3: Schematic of a Powder Diffractometer 14

Figure 4: Qualitative Comparison of PTX, INT, 3M and 3MA 26

Figure 5: Qualitative Comparison of 3M, 3MT and NAS 27

Figure 6: 2D PCA of 3M(1), 3MT(2) and NAS(3)..... 28

Figure 7: 2D CVA of 3M(1), 3MT(2) and NAS(3). Angle between axes=79.2 29

Figure 8:2D CVA of first 4 PCs of 3M(1), 3MT(2) and NAS(3)..... 30

Figure 9:2D CVA of all 3M, 3MT and NAS rolls..... 31

Figure 10:2D CVA of 3MA(1), 3MB(2), 3MC(3), 3MD(4) 32

Figure 11: 2D CVA of 3MB(1), 3MC(2), 3MD(3) 33

Figure 12: 2D CVA of 3MTA(1), 3MTB(2), 3MTC(3), 3MTD(4)..... 34

Figure 13: 2D CVA of 3MTA(1), 3MTC(2), 3MTD(3)..... 35

Figure 14: 2D CVA of NASA(1), NASB(2), NASC(3), NASD(4)..... 36

Figure 15: 2D CVA of NASB(1), NASC(2), NASD(3) 37

Figure 16:2D PCA of 3MA(1), 3MB(2), 3MC(3), 3MD(4)..... 38

Figure 17:2D CVA of 3MA(1), 3MB(2), 3MC(3), 3MD(4) 38

Figure 18:2D CVA of 3MB(1), 3MC(2), 3MD(3) 39

Figure 19: 2D CVA of 3MA(1), 3MC(2), 3MD(3) 40

Figure 20:2D PCA of 3MTA(1), 3MTB(2), 3MTC(3), 3MTD(4) 41

Figure 21:2D CVA of 3MTA(1), 3MTB(2), 3MTC(3), 3MTD(4)..... 41

Figure 22: 2D CVA of 3MTA(1), 3MTC(2), 3MTD(3)..... 42

Figure 23: 2D CVA of 3MTA(1), 3MTB(2), 3MTD(3) 43
Figure 24: 2D PCA of NASA(1), NASB(2), NASC(3), NASD(4) 44
Figure 25: 2D CVA of NASA(1), NASB(2), NASC(3), NASD(4) 44
Figure 26: 2D CVA of NASB(1), NASC(2), NASD(3) 45
Figure 27: 2D CVA of NASA(1), NASB(2), NASC(3) 47
Figure 28: Summary of quantitative comparison results 48
Figure 29: 2D CVA of 3MTA(1), 3MTB(2), 3MTC(3), 3MTD(4), small 3MTB(5)..... 49
Figure 30: 2D CVA of 3M(1), 3MT(2), NAS(3), small 3MTB(4)..... 50
Figure 31: 2D PCA of PE peaks, 3M (1), 3MT(2), NAS(3), 3MTB backing only(4)..... 51
Figure 32: 2D CVA of PE peaks, 3M (1), 3MT(2), NAS(3), 3MTB backing only(4)..... 52
Figure 33: 3MTB, backing only, perpendicular vs parallel 53
Figure 34: Group 1: A,E,I 55
Figure 35: Group 2: C,H,N,Q,R..... 56
Figure 36: Group 3: F,K,O,P 56
Figure 37: Group 4: G,L,M..... 57
Figure 38: 2D PCA of A(1), E(2), I(3) 58
Figure 39: 2D CVA of the first 5 PCs (A,E,I) 58
Figure 40: 2D PCA of C(1), H(2), N(3), Q(4), R(5)..... 60
Figure 41: 2D CVA of the first five PCs (C,H, N, Q, R)..... 60
Figure 42: 2D PCA of C(1), Q(2), R(3)..... 61
Figure 43: 2D CVA of the first five PCs (C,Q,R) 62
Figure 44: 2D PCA of H(1) and N(2) 63
Figure 45:2D CVA of the first 5 PCs (H, N) 63

Figure 46: 2D PCA of F(1), K(2), O(3), P(4) 64

Figure 47: 2D PCA of K(1), O(2), P(3) 65

Figure 48: 2D CVA of the first 3 PCs (K,O,P) 65

Figure 49: 2D PCA of G(1), L(2), M(3) 67

Figure 50: CVA of the first 5 PCs (G,L,M) 67

Figure 51: 2D PCA of H(1), N(2), Q(3) 69

Figure 52: 2D CVA of the first 3 PCs (H,N,Q) 69

Figure 53: 2D PCA of C(1), J(2), R(3) 70

Figure 54: CVA of the first 5 PCs (C,J,R) 71

Figure 55: Qualitative comparison of C,J,R 72

Figure 56: Summary of Blind Verification Results 73

Figure 57: Recommended XRD Comparison Scheme 75

Table of Tables:

Table 1: Hold-one-Out of 2D PCA, all three tape types 28

Table 2: Hold-one-Out of 2D CVA, all three tape types 29

Table 3: Hold-one-Out of 2D CVA of PCs, all three tape types 30

Table 4: Hold-one-Out of 2D CVA (3MA, 3MB, 3MC, 3MD) 39

Table 5: Hold-one-Out of 2D CVA (3MTA, 3MTB, 3MTC, 3MTD) 42

Table 6: Hold-one-Out of 2D CVA (NASA, NASB, NASC, NASD) 45

Table 7: Hold-one-Out of 2D CVA (NASB, NASC, NASD) 46

Table 8: Hold-one-Out of 2D CVA (A,E, I) 59

Table 9: Hold-one-Out of 2D CVA (C, Q, R) 62

Table 10: Hold-one-Out of 2D CVA (K, O, P) 66

Table 11: Hold-one-Out of 2D CVA (G, L, M) 68

Table 12: Hold-one-Out of 2D CVA (H, N, Q) 70

I. Context of this Study

Forensic science in and beyond the courtroom

Forensic science is most often associated with the use of information from examinations in court to support or refute guilt or innocence. In this role, forensic science provides the criminal justice system with additional information to consider in their decision making processes.

The results of forensic examinations can also be used to provide information to the investigation, both by suggesting avenues of investigation and by excluding suspects or hypotheses. It should be noted that many examination results and conclusions that are not sufficiently discriminating for use as evidence in court can nevertheless be extremely useful in the investigative stage.

The types of information forensic science examinations provide can be divided into four types (see R.Cook et al 1998 and Ingman & Rudin 2002):

Inclusive- substantiate or confirm links between suspects, victims, items and/or scenes

Exclusive-refute links between suspects, victims, items and/or scenes

Reconstructive- substantiate or refute the actions and/or sequence of actions that have taken place

Classifying-qualitative and/or quantitative identification of materials or items

Forensic science data is produced from the collection and analysis of physical evidence found at crime scenes. Despite evidence of the benefits of applications of forensic data to the investigative and intelligence world, research and implementation of forensic science continues to focus primarily on its function as proof in courts of law. This not only deprives said investigative and intelligence applications from an added information source, it also renders a huge wealth of forensic information underexploited.

Although the concept of collecting and processing forensic data is by no means novel, modern technology provides us with databases and computer programs capable of storing, handling and sorting large amounts of increasingly complex data, allowing these old concepts to be realized more effectively and on a larger scale.

Some data, such as DNA and fingerprints can provide a relatively strong link between people, objects and places on their own and are routinely collected in databases for use. Other sources of data such as shoeprints, paints, tool marks, and fibers are less systematically exploited. These are abundant on crime scenes, less expensive to process, and can provide significant information. Even if a particular piece of transfer evidence cannot provide conclusive enough inference to be useful as ultimate proof in a court of law, the information it provides can still be put to very good use in an investigative or intelligence setting.

Forensic data can be used to identify and distinguish between "crime phenomena" (similar modus operandi used by several groups; e.g. a new forgery method) and "crime series" (crimes committed by the same person/group of people, which could include one or more modus operandi). Both information suggesting a trend/pattern in modus operandi

used in general by many criminals and information suggesting a trend/pattern implying the work of a serial criminal/crime group can be a useful addition to crime intelligence and can also be used to guide policy directions and decisions.

In order to be able to properly evaluate and interpret forensic data from both individual forensic examinations and from databases containing data from multiple examinations, it is important that the analysis and examination methods used are scientifically validated. In the case of duct tape analysis, this involves determining to what extent various analysis alternatives distinguish between different potential sources of the tape. It is this body of knowledge to which the current research work has added. Besides being part of the foundation of quality and best practices in forensic science, this scientific method evaluation also fulfills part of the pre-requisites for the results of the examination being admissible as evidence in courts of law.

Crime and the use of duct tape

The development of duct tape has been attributed to the Johnson & Johnson Permacel division who created it during World War II for use as a water resistant sealing tape for ammunition cases. They used a rubber-based adhesive in order to increase the water resistance of the tape and added a fabric scrim to add strength to the backing.

Duct tapes are an increasingly important class of forensic evidence. Duct tape is ubiquitous in modern day society. In conjunction with criminal activities it is mainly used in packaging of contraband, construction of improvised explosive devices, and to bind or

gag victims. Duct tapes are the most frequently encountered tape evidence in the FBI lab (M.J. Bradley et al 2006) and both the Federal Bureau of Investigation (FBI) and European Network of Forensic Science Institutes (ENFSI) have and maintain duct tape databases.

Forensic analysis of duct tapes has two main aims. Comparing physical and chemical characteristics can help determine how likely it is that two or more tape samples come from the same roll of tape. This can help in proving or disproving links between suspects, victims and crime scenes, both in order to elucidate the events of a single crime or in order to link different crimes to each other. In addition, comparing the characteristics of an unknown tape sample to a database of known tape samples can provide information for the investigative process. The FBI Laboratory analyzes duct tape in both comparative examinations and for sourcing purposes (A. Hobbs et al 2007).

II. Statement of the Problem and Literature Review

Duct tape composition

Pressure sensitive tapes are generally composed of four different layers. Starting from the non-adhesive side, these layers are the release coating, the backing, the primer and the adhesive. Duct tapes also feature a scrim layer between the adhesive and the backing. The scrim is a fabric reinforcement layer composed of cotton, polyester, or a blend. The threads running along the length of the tape are called the warp and the threads woven through the warp are knows as the weft. The warp and weft layers of the

scrim can also have different compositions. The release coating, composed of long chain alcohols or cellulose esters, assist in reducing unwind tension and preventing the tape from sticking to itself when on a roll. The backing layer serves as a support for the adhesive, and is usually based on polyester, polyethylene, cellophane, polypropylene or polyvinyl chloride. Primers such as nitrile rubbers, chlorinated rubbers or acrylates help attach the adhesive to the backing. The pressure sensitive adhesives are based on polymers such as natural or synthetic rubbers, which are combined with tackifying resins and hydrogenated resins. Pigments and additives are added to the backing and adhesive layers in order to achieve the desired tape characteristics and appearance.

Common duct-tape construction consists of a polyisoprene-based adhesive, scrim, and a polyethylene backing (J. Johnston & J. Serra 2005). The use of multilayered polyethylene backings has become common practice in recent years (A. Hobbs et al 2007).

Manufacturing process

The manufacturing process involves three steps, coating, drying and slitting. Coating is the process of combining the backing layer with the scrim and adhesive, drying involves the partial drying of the adhesive, and slitting is the cutting and winding of the tape onto rolls for the final product.

There are a variety of different coating methods, all of which involve different configurations of rollers. The polymer backing is added either in solid sheet form or as a

liquid. The adhesive is added either melted or mixed with a solvent, though solvent coating is becoming obsolete due to the toxicity of the solvents and environmental impact of waste generation. The scrim is rolled in between the two layers.

Drying involves the cooling and/or drying of the tape and preparing it for slitting by adding the release coating to the outer side of the backing layer. The tape is then cut into the required widths and wound onto the tape holder in the slitting process.

Polyethylene orientation and crystallinity

The polymer used in the backing layer of duct tapes is polyethylene. Polyethylene is a semi-crystalline material. The crystalline component is influenced by many factors including microstructure, thermal history, processing and average molecular weight. As a result, slight variations in the manufacturing process may produce significant and detectable differences in the crystallinity of the product. X-ray diffraction is routinely used in polymer science to determine the crystallinity of polymers as well as the orientation of the crystalline fraction.

All of the manufacturing steps and the process of transferring the tape from one apparatus to another involve the tape being asserted to a variety of temperature changes and pressure from the rolls that the films and tape are carried on.

The x-ray diffraction pattern of crystalline polymers contains peaks characteristic of the structure of the polymer and a broad diffraction halo. The halo is due to lattice

defects in highly crystalline polymers and discrete noncrystalline regions in low crystallinity polymers. Noncrystalline polymers show one to three broad maxima thought to indicate certain spacings occurring with a particularly high frequency in the polymer.

Research has already shown the usefulness of qualitative and quantitative XRD in the analysis of polyethylene plastic bags for forensic purposes. In one study, researchers were able to successfully distinguish between 99.2% of 33 white grocery bags indistinguishable by visual inspection using solely the degree of crystallinity of the polyethylene component, intensity ratios of the main polyethylene peaks and the peaks due to additives.(V. Causin 2007)

Mineral composition and quantity

Even where FTIR and SEM/EDS can be used to identify the mineral component by elemental analysis, XRD has shown to be a preferred method for distinguishing between polymorphs (e.g. those of titanium dioxide) (P.C. Lowe 2004).

The FBI Laboratory has used qualitative XRD analyses to identify several minerals, anatase, rutile, calcite, dolomite, kaolinite, talc and zincite in duct tape. There are others that appear less regularly. To the author's knowledge, no quantitative analyses of the mineral component have been published to date.

Existing methodologies and technology for analysis

The initial examination of duct tapes involves characteristics distinguishable by visual and microscopic examination such as width, thickness, scrim count, scrim twist, weave pattern, adhesive color, backing color and number of backing layers. Where the aim of the analysis is to determine not only if two or more tape pieces could have originated from the same roll, but the sequence in which pieces were attached to each other in the parent roll, matching of tape end features, viewing of the polymer backing between crossed polarizers and analysis of the yaw of the scrim can be used.

Further examination of the backing and adhesive layers usually involves IR examination of both sides of the backing and the adhesive layer as well as SEM/EDS and qualitative XRD. Analysis of the fiber component involves characterization by PLM and checking for fluorescence.

Where the objective of the analysis is the matching of duct tape ends to each other, surface features and striations as well as tear surface details are considered prior to the examination of the class characteristics (M.J. Bradley et al 2006).

Other analyses that have been explored include cathodoluminescence, X-Ray Fluorescence (XRF), Laser-Ablation Inductively Coupled Plasma Mass-Spectroscopy (LA ICPMS) and Isotope-Ratio Mass-Spectroscopy (IRMS). The adhesive, backing and scrim layers all tend to luminesce. Besides being used to classify the major inorganic fillers and pigments, cathodoluminescence can be used to observe layer structure, voids,

as well as filler/pigment particle sizes and distributions (C. Palenik & J. Buscaglia 2007 and C. Palenik 2006).

In the Netherlands, XRF has been used to characterize the minor and major components of the adhesive portion, though contamination tends to limit the cases in which it can be applied. LA ICPMS of whole tape (backing and adhesive layers) has been found to have similar discrimination power as Vis/FT-IR analysis, while the discrimination power of IRMS (2H/1H and 13C/12C) of the whole tape has been shown to provide slightly better discrimination than Vis/FT-IR analysis (S. Montero, W. Wiarda, P. de Joode & G. van der Pejl 2005).

The ENFSI tape database contains the following information for duct tapes from different European markets: width, thickness, color impression (l*a*b*colorspace description), IR spectrum of the backing, IR spectrum of the adhesive and a close up photograph of the scrim with the adhesive removed.(S. Becker 2007).

Statement of some current analytical problems

A variety of physical investigations and instrumental analyses are used to gather information for discrimination of tapes. Efforts to further distinguish tapes have centered on elemental analysis of the adhesive layer. The adhesive layers have more variation in composition than the backing layers, but they are also more sensitive to contamination and weathering effects. Many of the methods providing information about elemental

composition involve analyses that destroy the sample, which is undesirable as the size of forensic tape samples is often very limited.

Although the polymer and mineral composition of the backing may not vary as much as the adhesive component, the different production methods and manufacturing machinery may result in detectable differences in patterns of orientation of the mineral components and a difference in the orientation and crystallinity of the polymer component. The recent industry trend towards the use of multilayered backings is an added reason to expect more variation to be found in the backing layer. Also, IRMS analysis of packaging tapes found that, where the $\delta^{13}C$ measure of a whole tape sample was ambiguous, removal of the adhesive and $\delta^{13}C$ analysis of the polymer backing on its own allowed for further discrimination (J.G. Carter 2004).

Where a larger sample is available, physical properties such as scrim count, width etc can be used to discriminate between a large number of manufactures and brands. In cases where the sample size is limited or is not composed of the entire roll width of tape, this option is not available. In those cases in particular, the addition of one more non-destructive analysis method is very useful.

X-Ray diffraction

XRD involves aiming x-ray radiation at a sample and recording the resulting diffraction pattern. The diffraction pattern in XRD is essentially an interference pattern resulting from x-rays being reflected by lattice planes of a crystalline substance. Waves

being reflected by separate, repeating crystal planes will interfere constructively and remain in phase if the difference between the distances they travel is equal to an integer multiple of the incident wavelength. These waves will appear to be reflected. Where the difference between the distances they travel is not equal to an integer multiple of the incident wavelength, destructive interference occurs and little or no waves will appear to have been reflected. The constructive interference that produces the diffraction patter can be summarized by the Bragg law: $2\ d \sin\theta = n\ \lambda$, where d is equal to the distance between the crystal planes, θ is the angle of incidence and λ the wavelength of the incident radiation.

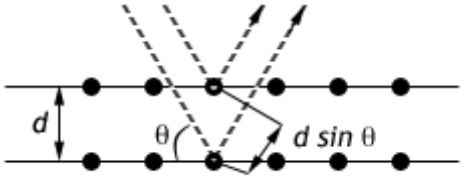

Figure 1: Diffraction of X-Rays in a lattice

In XRD, the angle of the incident radiation is changed in order to vary the distance that the waves travel to various crystal planes. If the wavelength is kept constant and known, cycling theta through a known set of angles and interpreting the resulting diffraction pattern allows us to calculate d, which is intrinsic to the lattice structure of the substance being analyzed.

The orientations and interplanar spacing of the crystal planes are described by three indices, h, k and l. If you call the three axes of the unit cell of the crystal a, b and c; a given set of planes with indices h, k, l cut the a-axis of the unit cell in h sections, the b-axis in k sections and the c-axis in l sections. Planes parallel to the axis are denoted with a zero. These indices are written in brackets after the corresponding 2θ angle. For example, to denote that the polyethylene peak at 21.6 2θ is the reflection of an h1, k1, l0 plane, one would write 21.6 (1 1 0).

XRD results are commonly displayed in a 2D graph with the 2θ angle on the x-axis and the intensity in counts per second on the y-axis, or in table format listing the 2θ angle and the corresponding d-spacing, peak height and peak area. The 2θ angle of the diffraction is based on the d-spacing while the intensity of the peak is affected by the number of planes parallel to the sample surface the type and location of atoms in the unit cell and thermal vibrations. The width of the peaks is affected by particle size and strain, but stacking faults and layering effects can also affect the shape of the peaks.

XRD analyses can be subdivided into two categories, single crystal and powder diffraction. Single crystal diffraction is used mainly to determine structural information of a particular crystal, namely the unit cell, cell dimensions and positions of atoms within the lattice. It is performed on a single crystal of approx 50—250 microns mounted on thin glass fibers attached to goniometer heads. Single Crystal XRD systems usually contain 3 or 4 goniometers. The goniometers are used to change the geometry of the incident rays, the orientation of the centered crystal and the detector in order to attain all possible diffraction directions of the lattice.

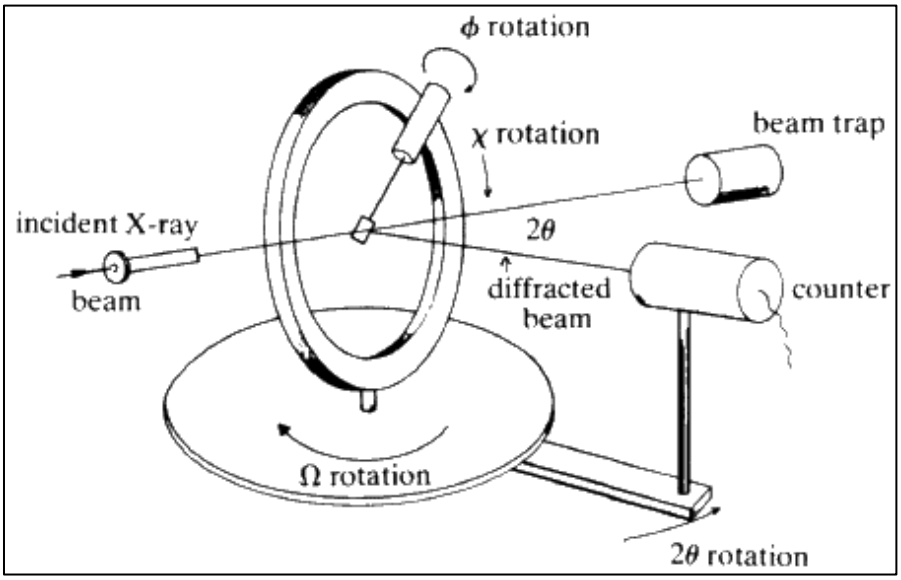

Figure 2: Schematic of a 4-circle single-crystal diffractometer[1]

Powder diffraction analyses multiple crystals and is used mainly for characterization of crystalline materials or quantitative determination of crystalline components. The sample is ground and loaded onto a holder to produce a uniform layer. Grinding the sample finely and minimizing preferred orientation effects is an integral part of sample preparation for phase identification and quantification purposes, as it ensures that the facets parallel to the sample surface contain a representation of all of the existing crystal planes. For analysis of non-powder samples, orientation effects can provide a further dimension of information. The incident X-Ray beam is stationary while the

[1] Image courtesy of the International Union of Crystallography www.iucr.org

sample is rotated to change the angle of incidence (θ) and the detector rotated into the appropriate position to catch any diffracted X-Rays (2θ).

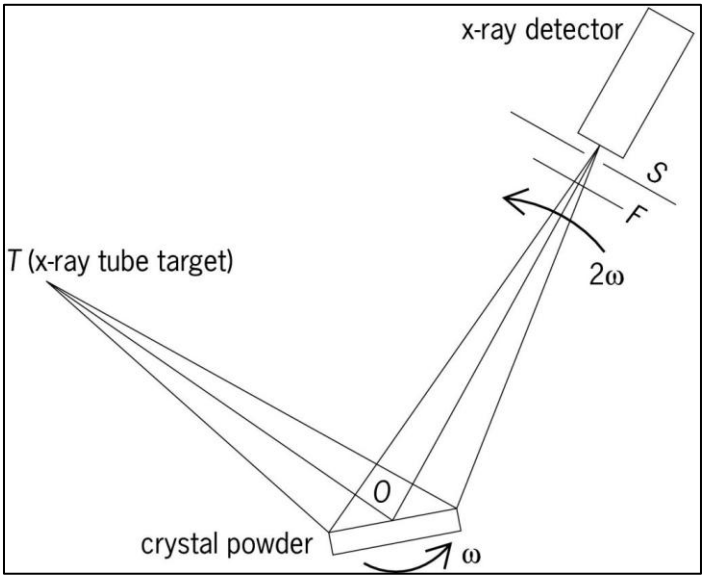

Figure 3: Schematic of a Powder Diffractometer[2]

XRD in forensics

Since XRD is non destructive and applicable to most materials, it has great potential forensically. Interpretation of complex diffractograms from multiple components and interference from broad diffraction bands caused by low crystallinity

[2] Image gourtesy of the Free Dictionary

components are two factors that can limit the applicability of XRD for analysis to materials.

XRD has been used to analyze a variety of materials from metals and alloys to paints, papers, pigments, cosmetics, minerals, fibers, soils, building materials, degraded bone material, cremains, plastics and polymers, soaps and detergents, automobile underseals, explosives and gunshot residues (D.F. Rendle 2003 and M. Kotyrly 2006). It is also used in the identification of 'unknown' samples, such as white powders.

In soil analysis, XRD is particularly well suited for the identification of minerals in the clay fraction (Interpol 2001). In paper characterization, XRD is used to determine the fillers and the degree of cellulose crystallinity. In pigment and paint analysis, it is used for characterization and comparison of transfer and contact samples as well as in artwork authentication. For analysis of both illicit drugs and pharmaceuticals, XRD has been used for differentiating between closely related compounds as well as for quantitative analysis of mixtures and confirming the polymorphs of pharmaceutical products.

XRD is used not only for the direct determination of organic and inorganic components of explosive and post blast residues, but also as a method to evaluate the success of separation and concentration of these residues (M. Kotryrly 2006). In combination with XRF, XRD has been used classify counterfeit coins (M. Hida 2001).

The usefulness of XRD coupled with IR for differentiating between white photocopy paper from different boxes has also been shown. Using the two methods,

researchers were able to differentiate between 19 similar types of office paper (V. Causin 2010).

III. Approach and Methodology

Introduction

This research project investigated the usefulness of qualitative and quantitative XRD analysis of duct tapes in distinguishing between tapes from different manufacturers and between different tapes from the same manufacturer. Limitations of specimen size were also explored.

Research protocol

The instrument that was used is a Rigaku Miniflex, which has a Cu target X-ray tube, a vertical goniometer with a 150cm radius, Ni Kβ suppression filter and a NaI(T1) scintillator detector with a Be window. The x-ray take-off angle is 6° and the datum or zero alignment angle 10°. The divergence slit is variable but interlocked with the theta axis in order to provide a constant irradiation width of approximately 11.5 mm regardless of the variation in the irradiation angle. The scatter slit and receiving slit are fixed at 4.2° and 0.3°, respectively and the soller slit has a divergence angle of +/- 2.5°.

The whole tape, backing and adhesive, was analyzed using an attachment which spins the sample to minimize orientation effects. When looking for evidence of

orientation effects in the backing, a stationary sample holder was used. Two types of sample holders were used, one made of aluminium and the second a silica low background holder.

The presence of background diffraction from the aluminum sample holder indicated that the beam penetrated the entire sample, even where the whole tape was analyzed. Though penetration through the entire sample by the x-ray beam is not desirable for traditional qualitative and quantitative XRD analyses, the nature of the sample did not allow for any opportunity to increase the sample thickness.

The variance in the depth of penetration due to instrumental factors, mainly any variation in the intensity of the x-ray beam, was considered to be mitigated by the fact that sample holder peaks were apparent in all of the samples and that the samples were run in random order and on various days. The variance in depth of penetration between tapes due to differences in sample characteristics was not considered as much of an issue since the aim of the experiment is to distinguish between samples based on their characteristics.

The tapes were also run on a low background holder. Peaks not seen with both the Al and the low background sample holders were not used in the quantitative comparison, in order to ensure that the effects seen could be attributed to the tape and not the sample holder.

The adhesive was removed from a number of tapes and the backing was run alone in order to determine which peaks should be attributed to the backing rather than the adhesive portion of the tape.

Comparisons were made between diffractograms from the same tape roll, those from different rolls of tape from the same manufacturer and those from tapes from different manufacturers.

Samples

Although duct tapes come in various colors, this research focused on the most common, the silver/grey tapes.

The quantitative analysis parameters used this study were based on extended analyses of three types of tape that could not be distinguished based on a qualitative comparison of their X-Ray diffractograms.

For each of those three types of tapes, four rolls were analyzed. Three of the four rolls were purchased from the same, unopened box at Home Depot[3] and one roll was purchased from an opened box in the same store six months later. Although it cannot be assumed that the first three rolls were from the same production batch, it was expected that the fourth roll purchased half a year later would not have been from the same batch as the first three. For each roll, 10 segments were analyzed along a 16 meter length of

[3] Home Depot at 40 W 23rd st, 10010 NY, NY

tape. The distance between the samples can be seen in Appendix A.

Qualitative comparison

Sample displacement is one of the most common sources of error in diffraction data. With the miniflex, the peak position is shifted 0.01 degrees along the 2θ axis (x-axis in the diffractogram) for every ~60μm of sample displacement. The 2θ value for the d-3.027 peak was used to guide the adjustment of the peak positions between diffractograms with the 'sample displacement adjustment' function in Jade. The peak of the 3MT9 sample on the low background holder was used as the zero-standard. The magnitude of these shifts can be seen in Appendix A.

Once the peak locations on the 2θ axis had been adjusted, qualitative comparisons were made by overlaying the diffractograms with the Jade software. Where there were no readily discernable peak position differences, the samples were grouped together for quantitative comparisons.

Quantitative Comparison

Quantitative comparisons involved statistical discrimination using Mathematica software. For clarity, the term 'scan' will be used to refer to individual diffractograms; the term 'sample', to the specific portions of tape analyzed; the term 'roll' to the rolls of tape analyzed; and the term 'type' to the make of tape in question. The term 'group'

varies depending on the what samples are being compared (rolls or types) but always denotes the units being compared to each other.

The statistical analysis methods used include Principal Component Analysis (PCA), Canonical Variate Analysis (CVA), Linear Discriminant Analysis (LDA) and Hold-one-Out verification. These methods are described in the sections below.

Data pretreatment

For quantitative analysis, the peak areas from the diffractograms were obtained with Jade software. The initial data processing was done in Excel and consisted of manually selecting the peaks that the samples of each group had in common. For the comparison between types, all twelve rolls were grouped together. For the within-type comparison, an additional three groups were considered, one for each type of tape. Thus, for the within-type comparisons, two different data sets were used.

This data was then imported into Mathematica. The peak areas were normalized by dividing all of the peak areas in each run by that of the d- 3.027 peak. The data was then arranged in a 2D data matrix where the rows contain data from specific scans and the columns contain the areas of specific peaks. As such, each number in the matrix represents the area under a specific diffraction peak in a specific scan. This data matrix as a whole will be referred to as 'X', and each number in the matrix as X_{ij}, where *i* and *j* are indicative of the scan and peak, respectively, that the number refers to.

No other data pretreatment such as centering or scaling of the data was done. Scaling was not done because we cannot assume that all variables should have equal statistical weight nor do we know how the weighting of the variables should be distributed. Centering was not done since we do not intend to quantitatively compare between models.

PCA

PCA is a multivariate method which assumes no prior grouping of samples. Linear combinations of the original variables are derived in order to provide a way to selectively delete variables and reduce the dimensionality of the original data set while keeping the most variance possible.

The variables (columns) in the new datamatrix are ordered according to the amount of variance they contain, allowing for the selection of variables which contain the majority of the variance. This means that deleting the lowest ranked variables will result in a minimum loss of information contained in the original datamatrix. This deletion of variables is what effectively reduces the dimensionality of the dataset. It should however be noted that on occasion these low variance variables may contain features required for successful discrimination between samples though they are not important to the overall structure of the data.

The linear combinations of the original variables that are derived, in matrix form, can be expressed as:

$$Z_{PC} = XA^T$$

where superscript T denotes the transpose of matrix **A**, which contains principal components as rows. The PCs were all normalized to unity. The matrix **A** was computed by diagonalizing the *p* x *p* (PC x PC) covariance matrix (**S**) of **X**:

$$SA^T = A^T\Lambda$$

Standard routines were used to determine the eigenvectors of **S** (the PCs in **A**) and the eigenvalues of **S** (the variance **Λ** of the PCs). The maximum likelihood covariance matrix, **S**, was computed as:

$$S = \frac{1}{n-1}\sum_{i=1}^{n}(X_i - \bar{X}) \otimes \left(X_j - \bar{X}\right)^T$$

where $\otimes$ is the Kronecker product of vectors.

CVA

The CVA method used is also known as Fisher linear discriminant analysis. It is a method that requires some prior grouping of samples. The analysis is based on the ratio of between group variance and within group variance. Besides being applicable to the original datamatrix, CVA can also be applied to the datamatrix derived with PCA.

Canonical variates are the geometrical axes which best separate the samples into discrete clusters when the data are projected onto them. The sample grouping provided to the model is used to guide the computation of the canonical variates.

Note that some variables are redefined here, i.e. that they are not the same as those defined in the previous section concerning PCA.

The CVs(**A**) and their eigenvalues (**Λ**) can be computed by diagonalizing the matrix $\mathbf{W}^{-1}\mathbf{B}$:

$$\boldsymbol{B} = \sum_{i=1}^{k} n_i \quad (\bar{X}_i - \bar{X}) \otimes (\bar{X}_i - \bar{X})^T$$

where **B** is the between-group variance

$$\mathbf{W} = \sum_{i=1}^{k} \sum_{j=1}^{n_i} \left(\bar{X}_{ij} - \bar{X}_i\right) \otimes (\bar{X}_{ij} - \bar{X}_i)^T$$

where **W** is the within-group variance

$\mathbf{X_{ij}}$ represents the *j*th scan in the *i*th group and $\bar{\boldsymbol{X}}_{\mathbf{i}}$ is the average of all of the scans in the *i*th group. The number of scans per group is denoted by $\boldsymbol{n_i}$ and $\otimes$ is the Kronecker product of vectors.

The eigenvectors of CVA are not necessarily orthogonal to each other because the eigenproblem for CVA, $W^{-1}\,BA^T = A^T\Lambda$, is not symmetrical. The angle between the CVs is indicative of how independent they are. The closer the angle is to 90, the more independent the CVs are, the closer the angle is to 0 or 180, the more collinear the vectors are.

LDA

LDA is a classification analysis technique that uses distance functions based on a Mahalanobis type metric to numerically discriminate between data in datamatrices. It also requires prior grouping of samples. It can be applied not only to the original datamatrix, but also to those derived with PCA and CVA.

LDA is a classification analysis technique that uses distance functions based on a Mahalanobis type metric to numerically discriminate between data in datamatrices. It also requires prior grouping of samples. It can be applied not only to the original datamatrix, but also to those derived with PCA and CVA.

LDA trains a set of linear functions to be able to assign a particular data pattern to a specific group. The discriminant function is constructed for a given group, *i*, as follows:

$$L_i(Y_i) = \bar{Y}_i^T S_{pl}^{-1} Y_j - \frac{1}{2} \bar{Y}_i^T S_{pl}^{-1} Y_i$$

The distance metric used is as follows:

$$D^2(Y_j) = \left(Y_j - \bar{Y}_i\right)^T S_{pl}^{-1} (Y_j - \bar{Y}_i)$$

where $\bar{Y}_i$ is the average scan of group i contained in the matrix being considered; Y_j is the scan being tested and S_{pl} is a pooled covariance matrix for all the groups:

$$S_{pl} = \frac{1}{n-k} \sum_{i=1}^{k} (n_i - 1) S_i$$

where S_i is the covariance matrix for group *i*.

The decision rule $\arg\max L_i(Y_j)$ is used to assign the test scan, Y_j, to the group, *i*, whose discriminant function yields the largest numerical value.

Once all of the discriminant functions have been calculated based on the provided groups, each scan is assigned to a group based on those functions. The number of correct and mistaken classifications based on the functions reflects the sample clustering in the datamatrix. This provides a useful measure for the amount of discrimination produced with PCA and CVA if the LDA is applied to the PCA and CVA datamatrices.

Hold –one-Out verification

A 'Hold-one-Out' verification analysis method for computing correct classification was used to provide an additional estimate of the classification performance of the LDA.

In Hold-one-Out verification, the data set is replicated using all but one of the original data vectors. The statistic, in this case LDA, is recalculated using the replicated, *n*-1, data set. That one 'held-out' data vector is then classified using the recalculated statistic. This holding-out process is repeated sequentially for each scan.

IV. Findings

Qualitative Comparisons: Results

Since there is a large variation of duct tapes available, and qualitative XRD is already used to differentiate between duct tapes, the qualitative comparisons in this project were geared towards identifying similar tapes suitable for quantitative analysis rather than cataloguing the variety available.

Several tapes which could be readily distinguished by simple visual qualitative comparison. For example, the difference between two types of 3M tapes, Intertape and Pattex below:

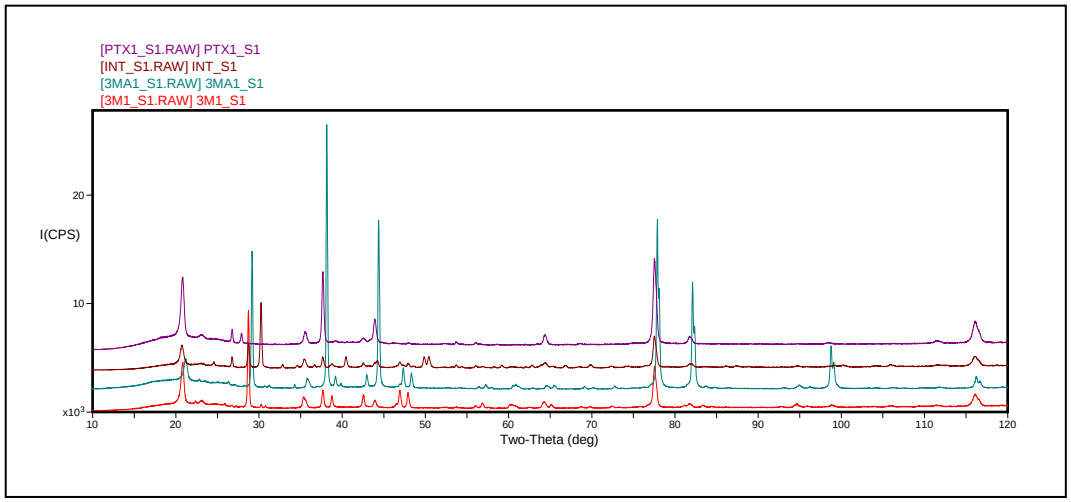

Figure 4: Qualitative Comparison of PTX, INT, 3M and 3MA

Out of the tapes qualitatively compared, three were not readily distinguishable . These were the 3M tape (3M), 3M Tough(3MT) and Nashua (NAS) tapes.

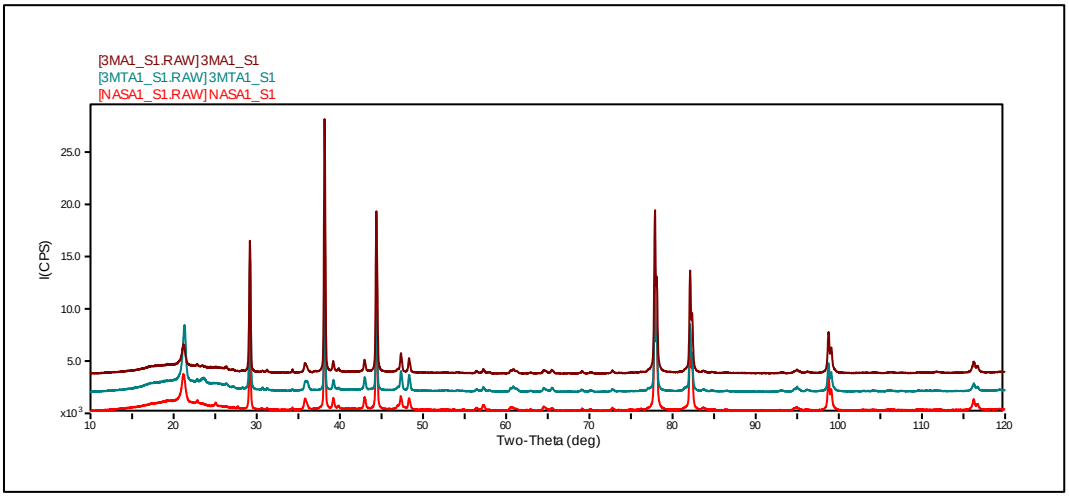

Figure 5: Qualitative Comparison of 3M, 3MT and NAS

Quantitative Comparisons: Results

Between-type comparisons:

The three qualitatively similar tapes were then further compared using quantitative analysis. Scans from four rolls of each of the types were used. A PCA of the scans of each roll was done in order to identify and discard any outliers. These results can be seen in Appendix B. 48 scans from 3M tapes, 50 from 3MT tapes and 50 from NAS tapes remained for the comparison. Peaks common to all scans from all twelve rolls were chosen for the quantitative comparison. This resulted in the use of 14 peaks for the comparison. (See Appendix C for a listing of the peaks). The data was imported into Mathematica for processing.

Comparison of the three tape types, 3M, 3MT and NAS:

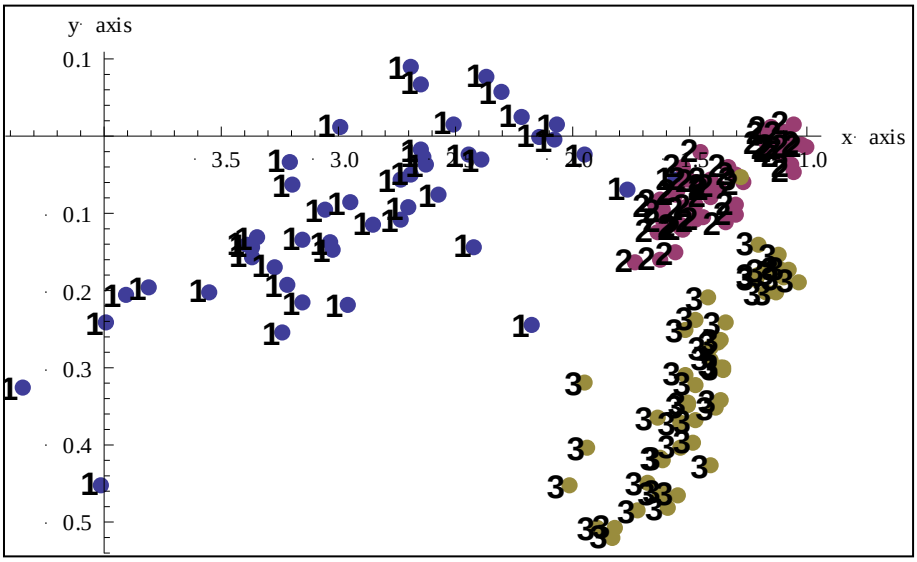

Figure 6: 2D PCA of 3M(1), 3MT(2) and NAS(3)

2D PCA	3M	3MT	NAS	% Misclassified
3M	44	4		**8.33**
3MT		50		**0.00**
NAS		2	48	**4.00**

Table 1: Hold-one-Out of 2D PCA, all three tape types

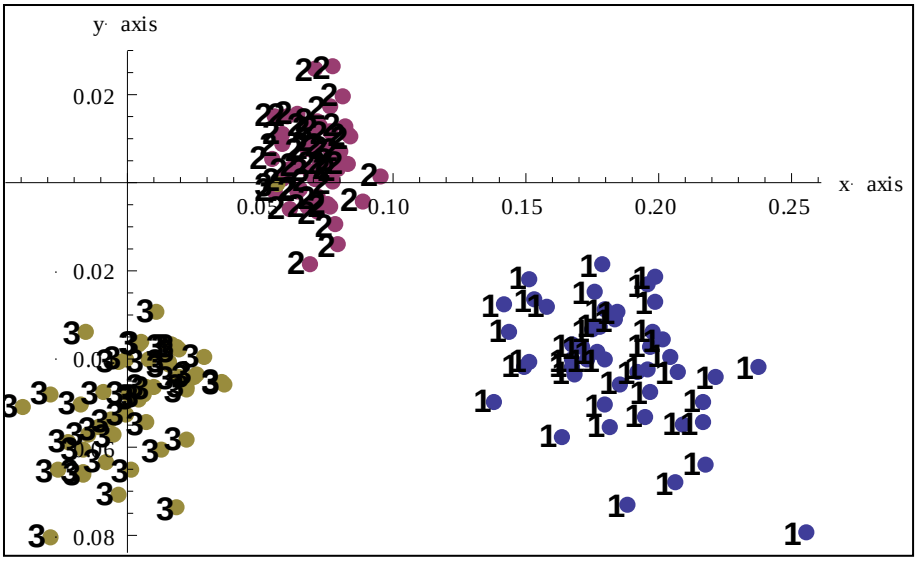

Figure 7: 2D CVA of 3M(1), 3MT(2) and NAS(3).
Angle between axes=79.2

2D CVA	3M	3MT	NAS	% Misclassified
3M	48			**0.00**
3MT		50		**0.00**
NAS		1	49	**2.00**

Table 2: Hold-one-Out of 2D CVA, all three tape types

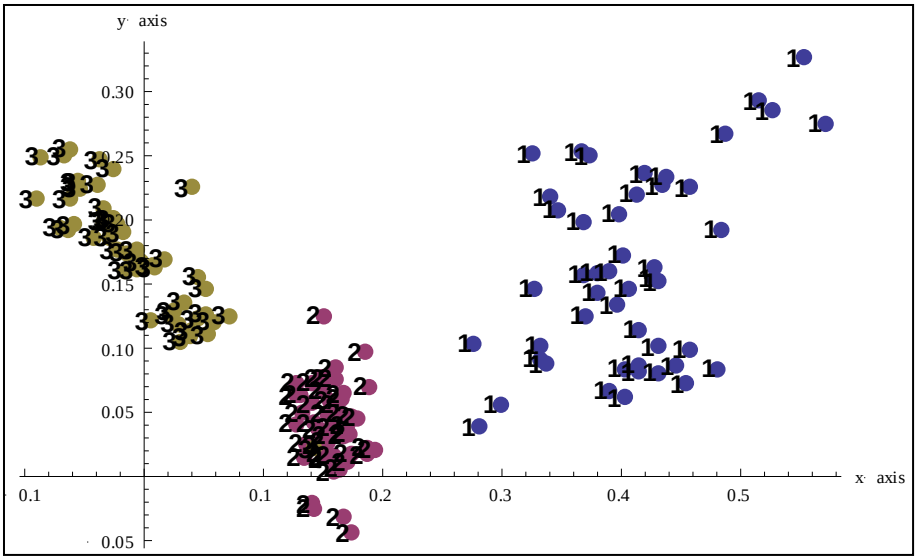

Figure 8:2D CVA of first 4 PCs of 3M(1), 3MT(2) and NAS(3)
Angle between axes=79.5

2D CVA of PCs	3M	3MT	NAS	% Misclassified
3M	45	3		**6.25**
3MT		50		**0**
NAS		1	49	**2**

Table 3: Hold-one-Out of 2D CVA of PCs, all three tape types

Despite some misclassifications in the verification of the classification, the three tape types can obviously be seen to cluster separately.

All twelve rolls were then labeled individually and the CVA analysis repeated. Since the CVA calculations are based on the user defined group label of each dataset, this allowed for a determination of to what extent the pre-defined grouping of the scans might affect the CVA results.

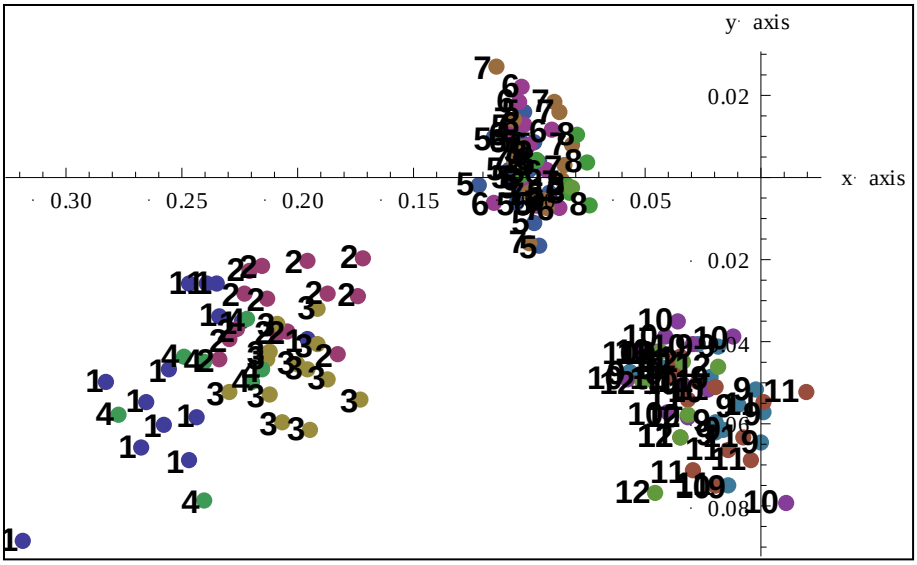

Figure 9:2D CVA of all 3M, 3MT and NAS rolls
Angle between the axes = 92.2

Hold-one-Out verification misclassified several data points, however only one sample was wrongly assigned to a roll of a different type. This suggests that there is more difference between the types than between the rolls, and that these differences and similarities are sufficient enough to overcome any effects from the user-defined grouping of the scans.

Within-Type Comparisons

Each one of the three types was then considered separately, using the same 14 peaks that were chosen for the between-type comparison, in order to see if the four rolls of each type could be differentiated using the same data.

3MA, 3MB, 3MC, 3MD:

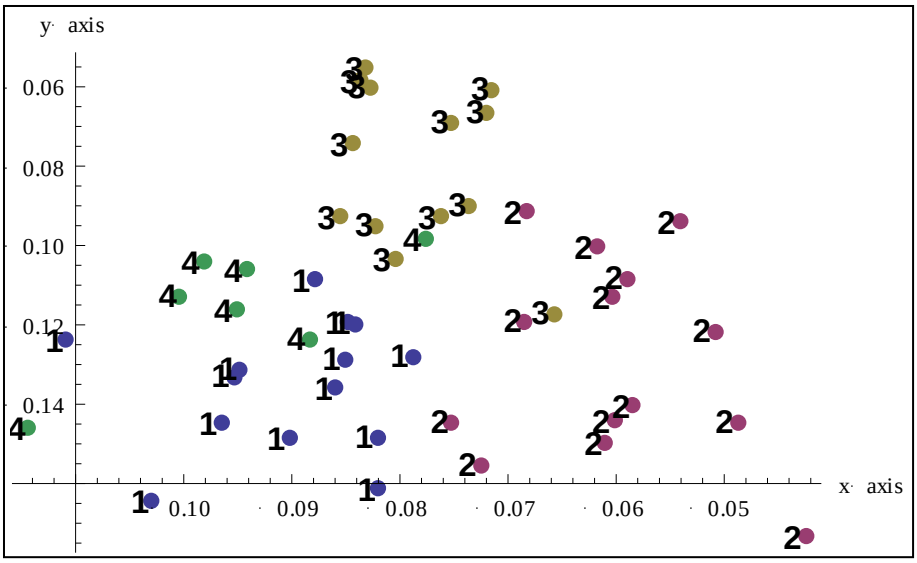

Figure 10:2D CVA of 3MA(1), 3MB(2), 3MC(3), 3MD(4)
Angle between the axes = 91.8

Though the scans from the same tape do show some tendency to group together, there are no obviously separate clusters to be seen. The Hold-one-Out verification misclassified two from group 1, two from group 2, one from group 3 and three from group 4.

Increasing to 3CVs did not result in any significant improvement, and Hold-one-Out verification results in a misclassification of two from group 1, three from group 2, one from group 3 and two from group 4.

Since 3MA seemed to overlap the most with the other three, 3MB, 3MC and 3MD were compared without 3MA to see if any clearer pattern would emerge.

3MB, 3MC, 3MD:

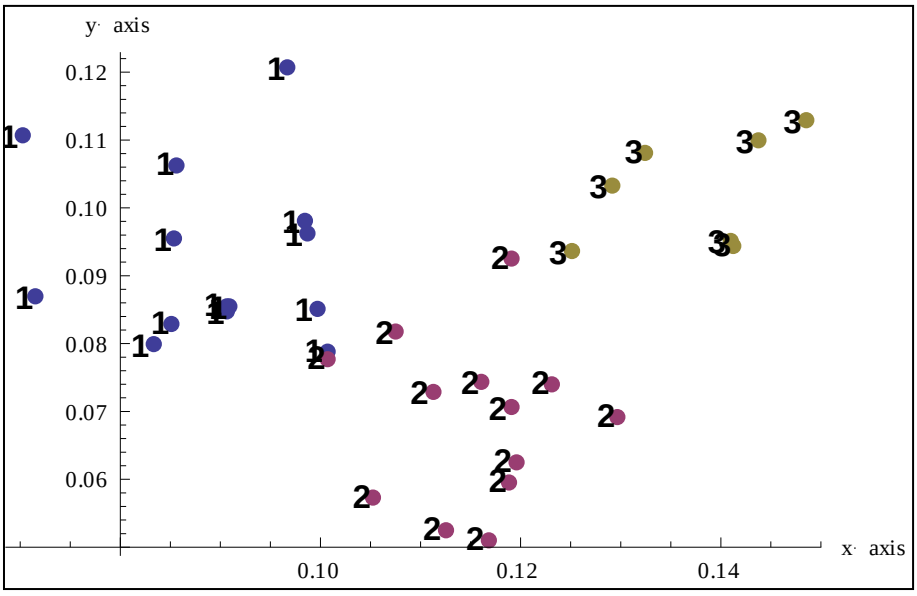

Figure 11: 2D CVA of 3MB(1), 3MC(2), 3MD(3)
Angle between axes = 52.0

Hold-one-Out verification results in one group 1 misclassified as group 2, one group 2 misclassified as group 3 and one group 2 misclassified as group 1. This suggests that groups 1 and 3 can be told apart.

Increasing to 3D CVs does not result in a change in the Hold-one-Out verification result.

3MTA, 3MTB, 3MTC, 3MTD:

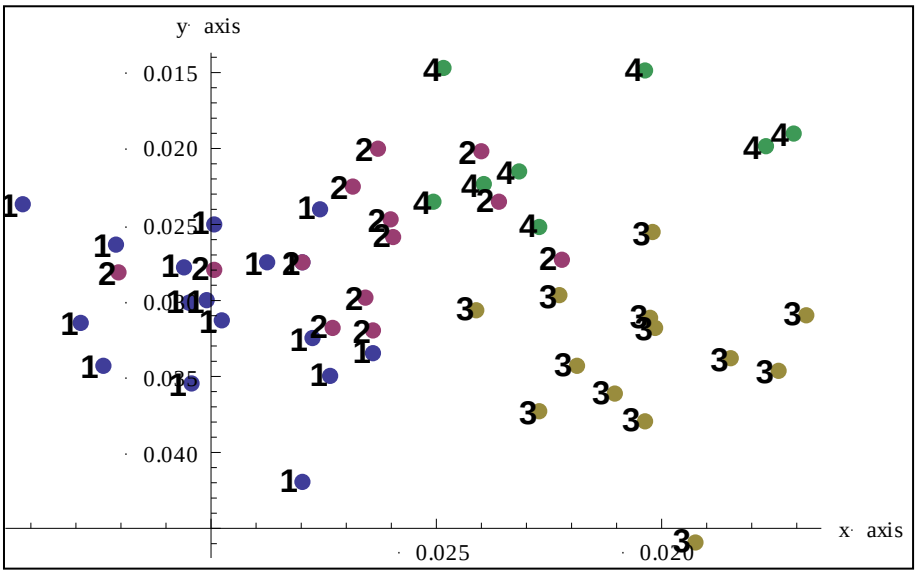

Figure 12: 2D CVA of 3MTA(1), 3MTB(2), 3MTC(3), 3MTD(4)
Angle between axes = 104.9

Hold-one-Out verification results in three group 1 misclassified as group 2, six group 2 misclassified as group 1 or 4 (three each), one group 3 misclassified as group 2, one group 3 misclassified as group 2 and one group 4 misclassified as group 2.

Since group 2, 3MTB, seems to overlap the most with the other three groups, 3MTA, 3MTC and 3MTD were considered separately.

3MTA, 3MTC, 3MTD:

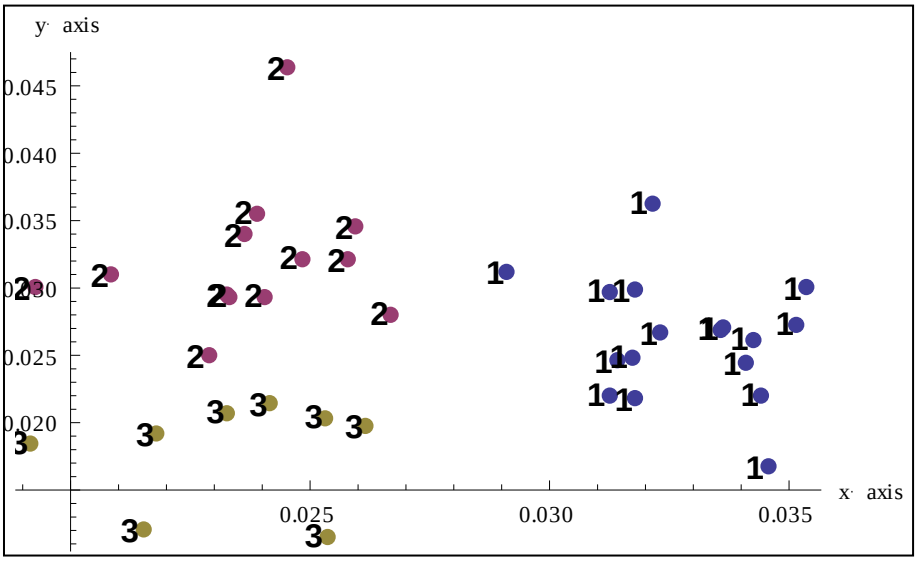

Figure 13: 2D CVA of 3MTA(1), 3MTC(2), 3MTD(3)
Angle between the axes = 108.2

Hold-one-Out verification resulted in one group 2 misclassified as a group 3. Increasing to 3CVs did not change the Hold-one-Out verification results. Group 1 can be distinguished from groups 2 and 3 but groups 2 and 3 are not readily separable.

NASA, NASB, NASC, NASD:

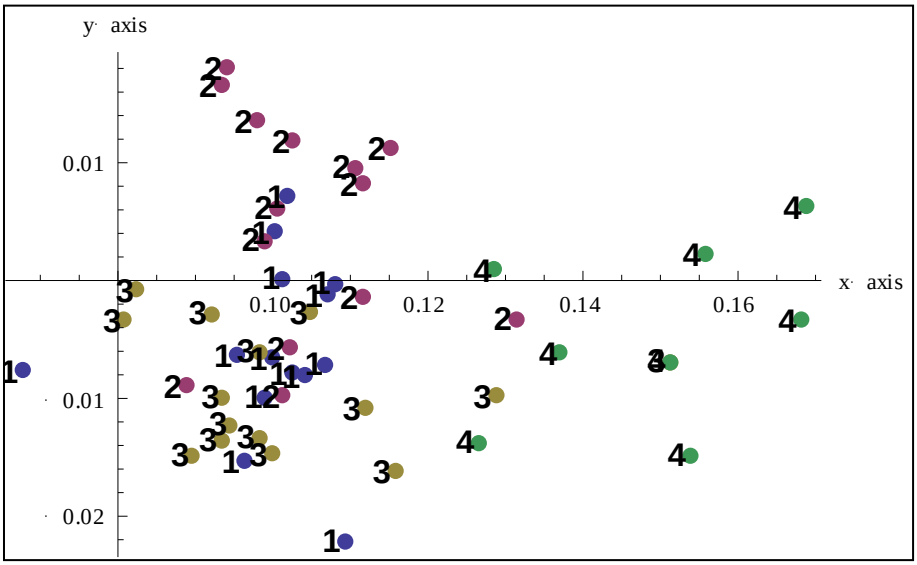

Figure 14: 2D CVA of NASA(1), NASB(2), NASC(3), NASD(4)
Angle between the axes = 83.0

Here again, there are no distinguishable clusters of datapoints to be observed. NASB, NASC and NASD were considered separately to see if any pattern would emerge without the interference of NASA.

NASB, NASC, NASD:

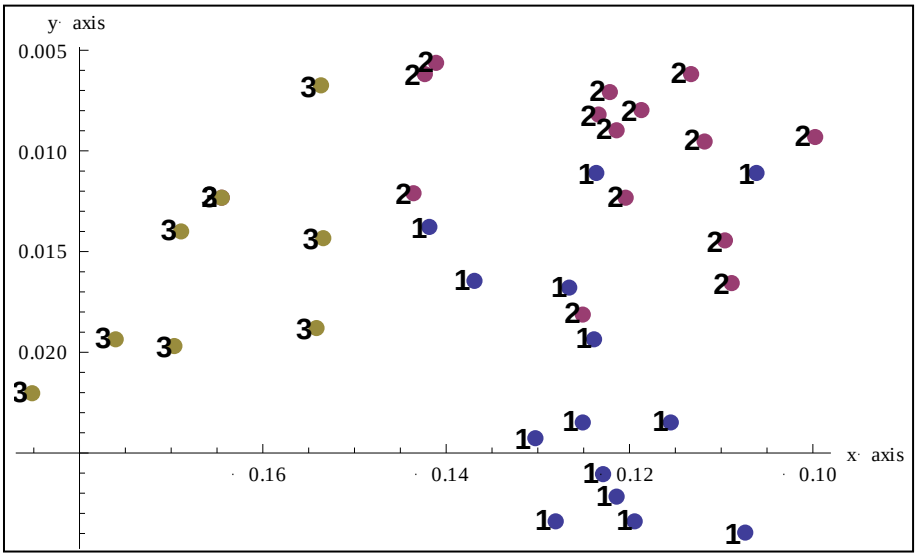

Figure 15: 2D CVA of NASB(1), NASC(2), NASD(3)
Angle between the axes = 77.5

Even though Hold-one-Out verification results in fewer misclassifications, there is still very little obvious clustering apparent and much overlap between all three groups.

Further Within-Type Comparisons:

The rolls within each type then also compared using only the peaks that were common to each one of the three types; i.e. the data processing was repeated starting from the selection of peaks common to all rolls from each type. This resulted in a different number of peaks for each type.

3MA , 3MB, 3MC, 3MD:

For these comparisons, 18 peaks were used. (See Appendix C for a peak list)

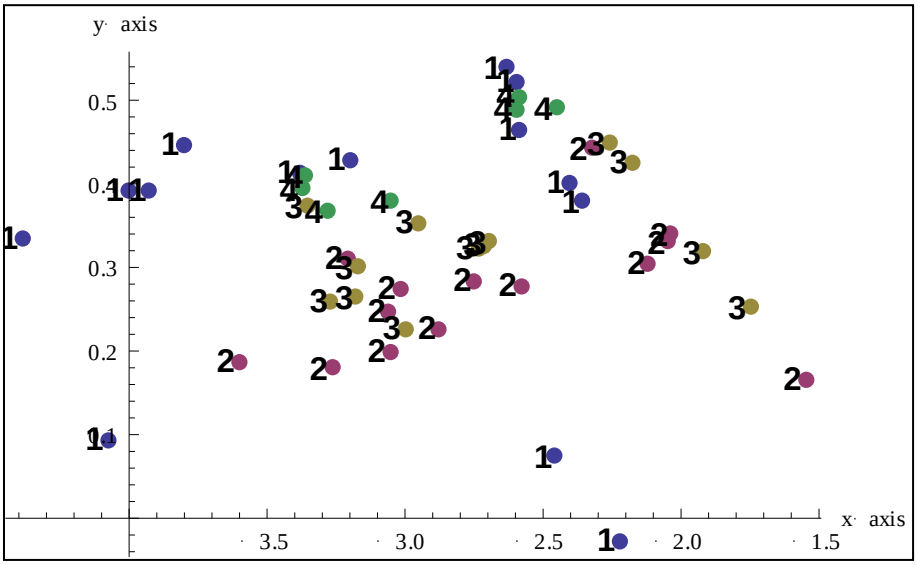

Figure 16:2D PCA of 3MA(1), 3MB(2), 3MC(3), 3MD(4)

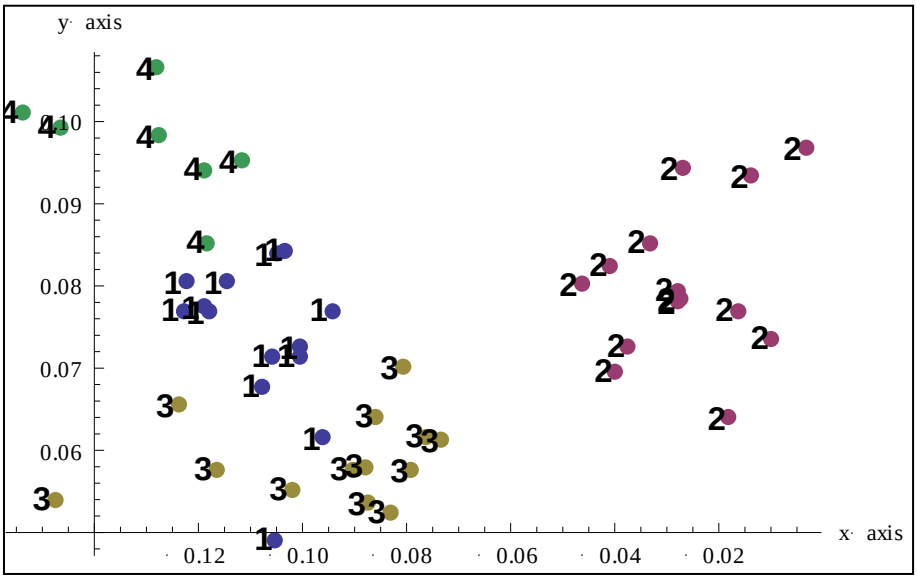

Figure 17:2D CVA of 3MA(1), 3MB(2), 3MC(3), 3MD(4)
Angle between axes = 105.9

2D CVA	3MA	3MB	3MC	3MD	% Misclassified
3MA	14		2		**12.5**
3MB		14			**0**
3MC	3		13		**18.75**
3MD	1			7	**12.5**

Table 4: Hold-one-Out of 2D CVA (3MA, 3MB, 3MC, 3MD)

Hold-one-Out verification resulted in two group 1 misclassified as group 3 as well as three group 3 and one group 4 misclassified as group 1. This suggests that groups 2, 3 and 4 can all be told apart. This can be seen more clearly by comparing 3MB, 3MC and 3MD without 3MA:

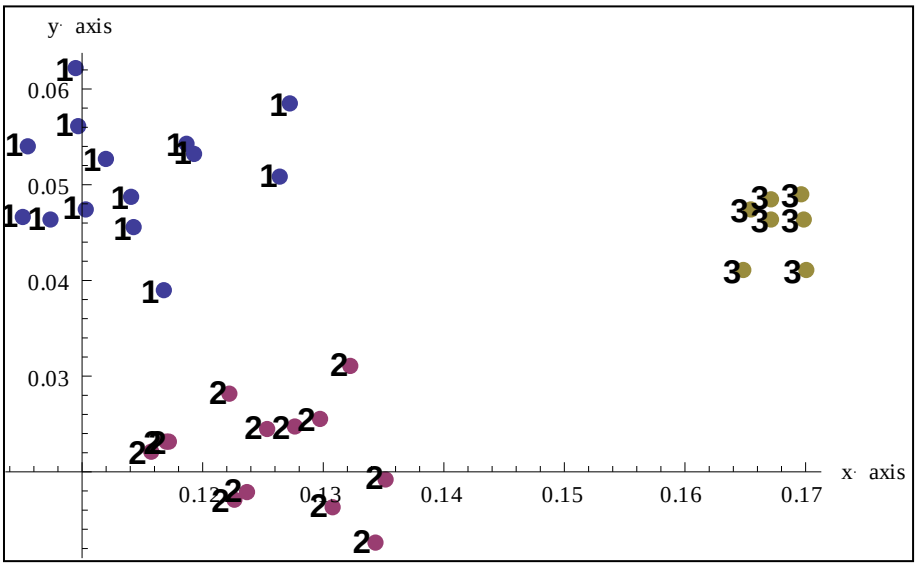

Figure 18:2D CVA of 3MB(1), 3MC(2), 3MD(3)
Angle between the axes = 48.3

Hold-one-Out and LDA verification resulted in no misclassifications. The clusters of datapoints are also visibly separate from each other, supporting the verification results.

3MA, 3MC and 3MD were then compared without 3MB to determine how well they could be differentiated.

3MA, 3MC, 3MD:

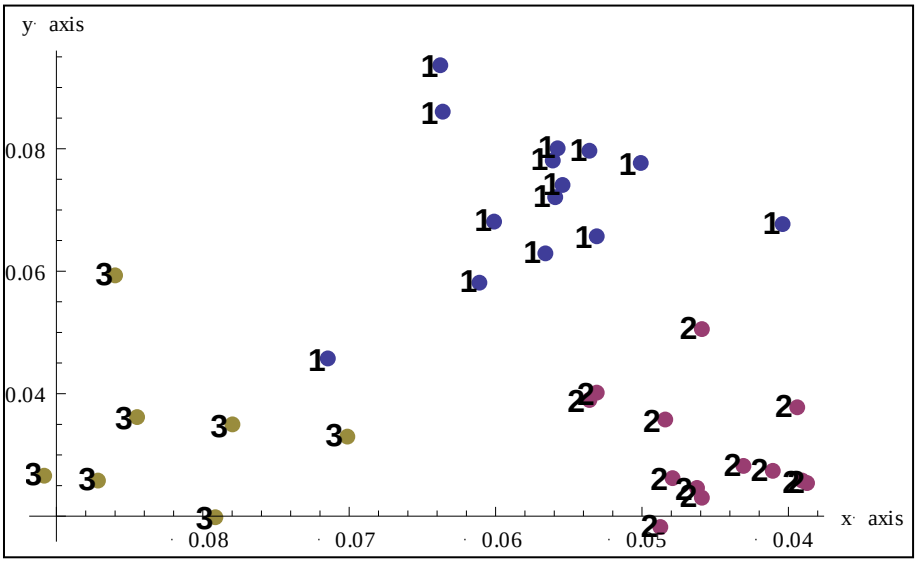

Figure 19: 2D CVA of 3MA(1), 3MC(2), 3MD(3)
Angle between axes=52.1

Here 3MC and 3MD can again be told apart but hold-one-Out verification misclassifies one 3MA sample as belonging to 3MC and another as belonging to 3MD so 3MA cannot be readily distinguished from either one of them.

In the case of the 3M tapes, 3MB can be distinguished from the three other tapes and 3MC from 3MD, but 3MA cannot be distinguished from 3MC or 3MD.

3MTA, 3MTB, 3MTC, 3MTD:

For these comparisons, 21 peaks were used. (See Appendix C for a listing of the peaks)

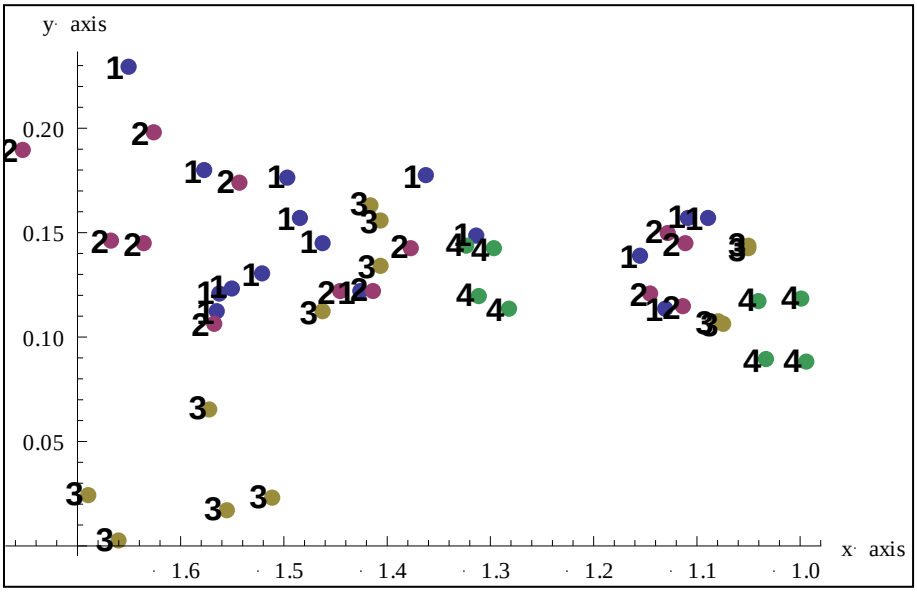

Figure 20:2D PCA of 3MTA(1), 3MTB(2), 3MTC(3), 3MTD(4)

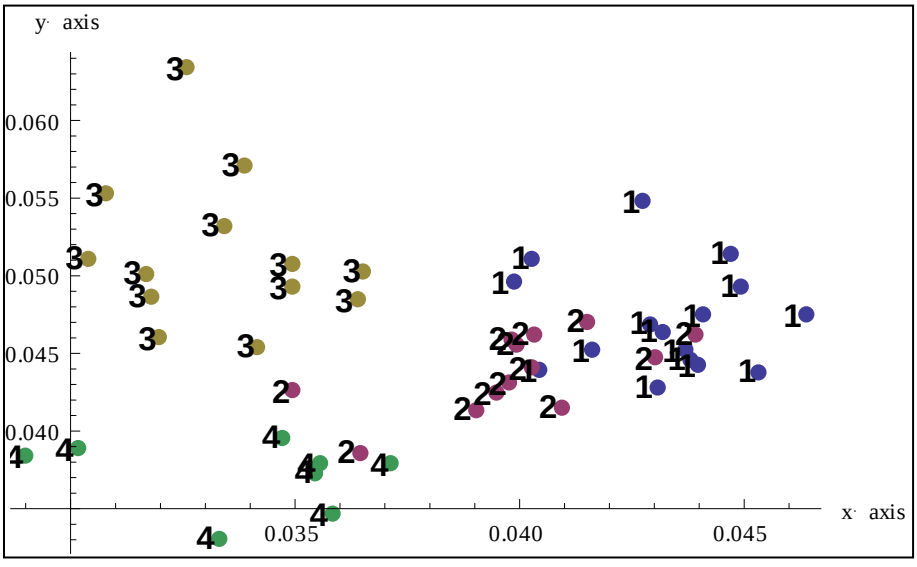

Figure 21:2D CVA of 3MTA(1), 3MTB(2), 3MTC(3), 3MTD(4)
Angle between axes = 87.9

2D CVA	3MTA	3MTB	3MTC	3MTD	% Misclassified
3MTA	13	3			**18.75**
3MTB	3	7		2	**41.67**
3MTC			13		**0.00**
3MTD				8	**0.00**

Table 5: Hold-one-Out of 2D CVA (3MTA, 3MTB, 3MTC, 3MTD)

Hold-one-Out verification results in three group 1 misclassified as group 2, three group 2 misclassified as group 1 and two group 2 misclassified as group 4. This means that groups 1, 3 and 4 can be told apart. This can be seen more clearly when comparing 3MTA, 3MTC and 3MTD without 3MTB:

3MTA, 3MTC, 3MTD:

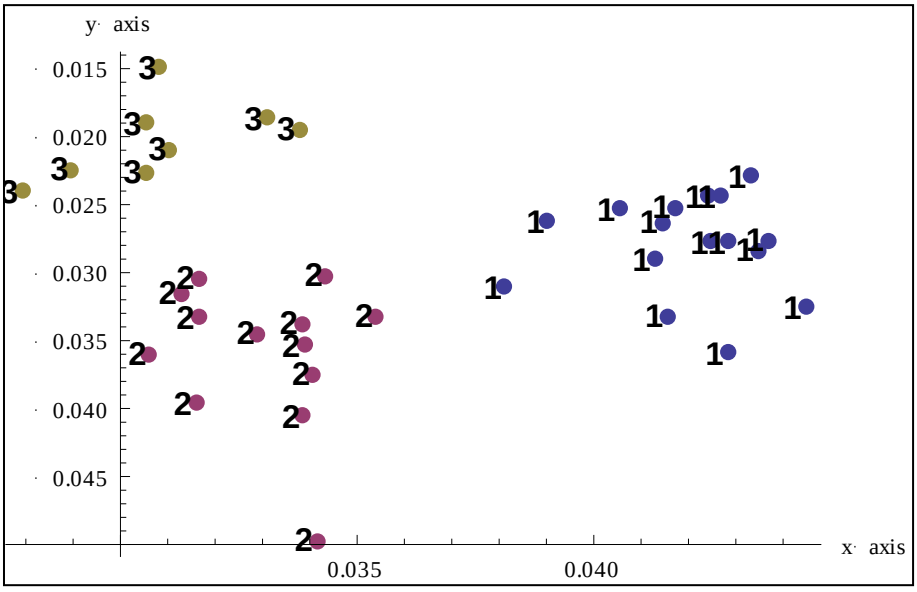

Figure 22: 2D CVA of 3MTA(1), 3MTC(2), 3MTD(3)
Angle between the axes = 84.1

Hold-one-Out and LDA verification resulted in no misclassifications, again, the three groups of datapoints form quite separate clusters.

3MTA, 3MTB and 3MTD were then compared without 3MTC to see if 3MTB could be distinguished from 3MTA and 3MTD.

3MTA, 3MTB, 3MTD:

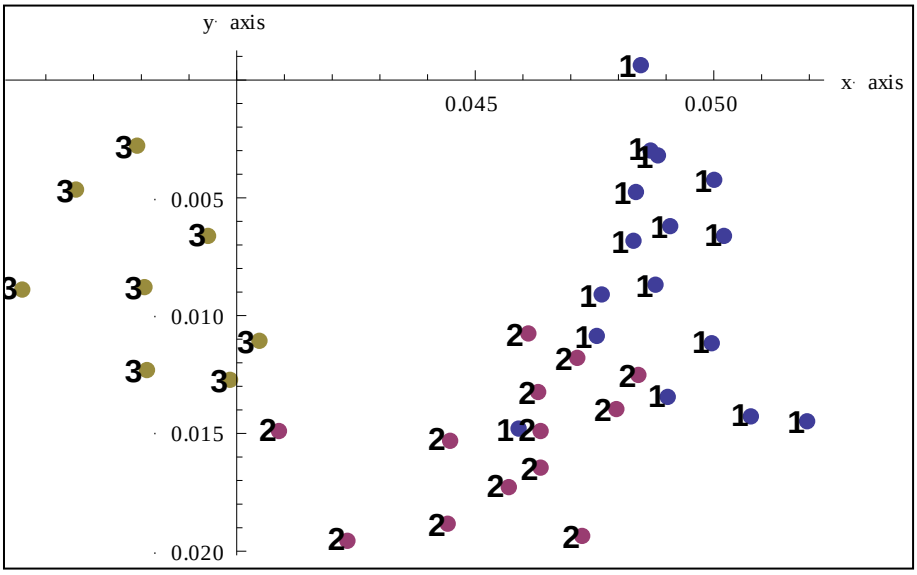

Figure 23: 2D CVA of 3MTA(1), 3MTB(2), 3MTD(3)
Angle between the axes = 112.5

3MTA and 3MTD can be readily told apart, but the datapoints from 3MTB do not seem to form a distinct cluster or to separate very well from 3MA and 3MD.

For the 3MT tapes, 3MC can be distinguished from the other three and 3MA from 3MD, but 3MB cannot be distinguished from 3MA or 3MD.

NASA, NASB, NASC, NASD:

For these comparisons, 19 peaks were used. (See Appendix C for a listing of the peaks)

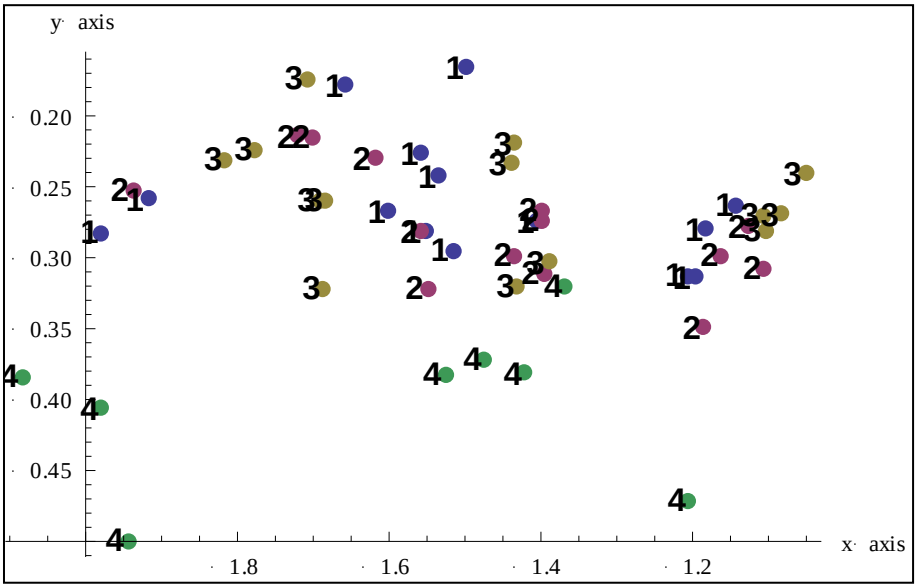

Figure 24: 2D PCA of NASA(1), NASB(2), NASC(3), NASD(4)

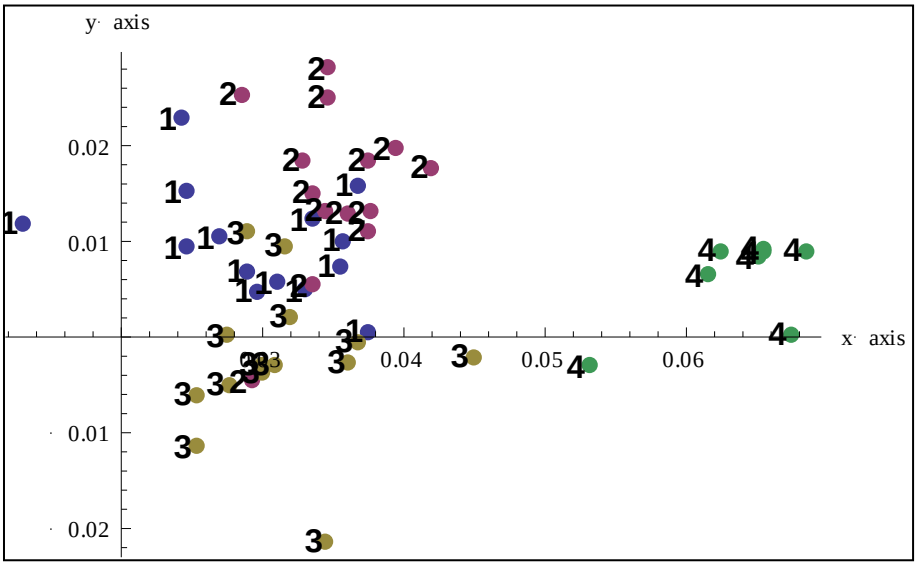

Figure 25: 2D CVA of NASA(1), NASB(2), NASC(3), NASD(4)
Angle between axes = 101.4

2D CVA	NASA	NASB	NASC	NASD	% Misclassified
NASA	8	5	1		**42.86**
NASB	1	12	1		**14.29**
NASC	1		13		**7.14**
NASD				8	**0.00**

Table 6: Hold-one-Out of 2D CVA (NASA, NASB, NASC, NASD)

NASD can be distinguished from the other three. Hold-one-Out verification resulted in six misclassified group 1, two misclassified group 2 and two misclassified group 3. NASB, NASC and NASD were compared separately to see if they could be distinguished without NASA.

NASB, NASC, NASD:

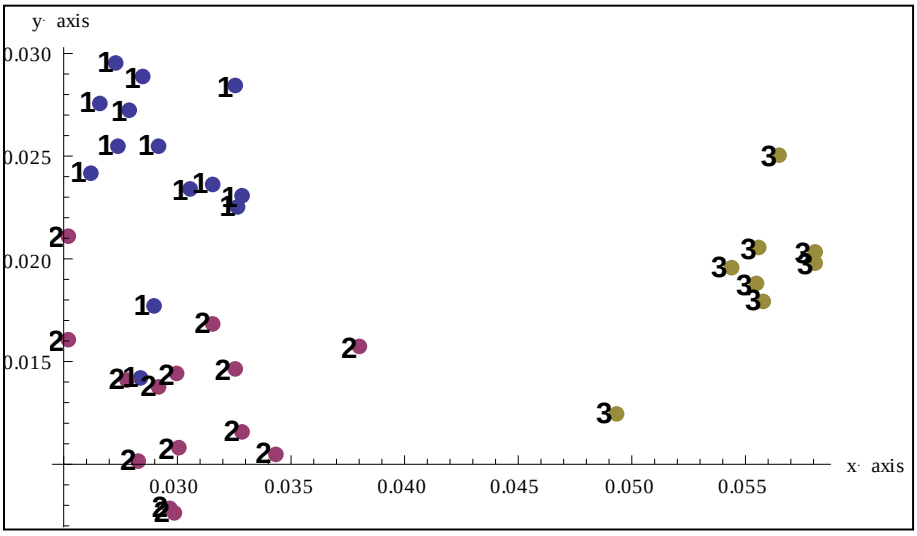

Figure 26: 2D CVA of NASB(1), NASC(2), NASD(3)
Angle between axes=133.4

2D CVA	NASB	NASC	NASD	% Misclassified
NASB	14	2		**12.50**
NASC	1	14		**6.67**
NASD			8	**0.00**

Table 7: Hold-one-Out of 2D CVA (NASB, NASC, NASD)

Hold-one-Out verification resulted in two group 1 misclassified as group 2 and one group 2 misclassified as group 1. Increasing to three CVs did not improve separation; the Hold-one-Out verification results remained the same. This suggests that NASD can be told apart from NASB and NASC but that NASB and NASC cannot be differentiated between.

Since NASD was so clearly separated from the other three tapes, NASA, NASB and NASC were compared without NASD.

NASA, NASB, NASC:

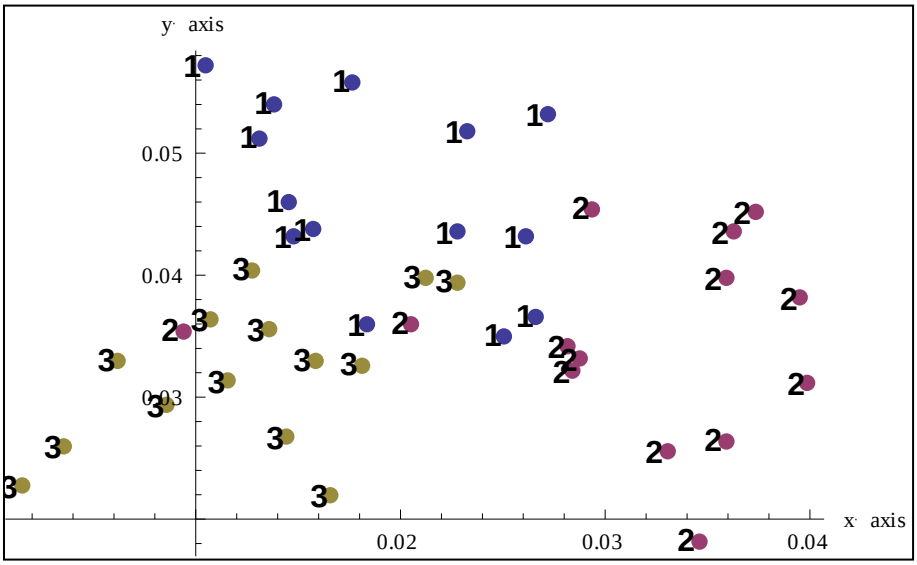

Figure 27: 2D CVA of NASA(1), NASB(2), NASC(3)
Angle between axes=98.8

Leaving out NASD did not result in any better resolution between the clusters of NASA, NASB and NASC.

For the NAS tapes, NASD can be distinguished from the other three, but NASA, NASB and NASC cannot be told apart.

Summary of Quantitative Comparison Results:

It was seen that all three types of tapes could be readily distinguished from each other. Given the tight clustering of the three groups, the separation between them, and the location of the one misclassified datapoint in the center of another cluster rather than in the periphery of the cluster; it can be discounted as an outlier. This is also supported by

the PCA of the NASD tape, where NASD2, which is the outlier datapoint, is placed on the periphery of the 2D graph. (See Appendix B)

When comparing rolls from the same type, rolls 3MB, 3MC and 3MD could be distinguished from each other, but roll 3MA could not be told apart from rolls 3MC and 3MD.

Rolls 3MTA, 3MTC and 3MTD could be distinguished from each other but roll 3MTB could not be distinguished from 3MTA or 3MTD.

For the Nashua tapes, only NASD could be distinguished from NASA, NASB and NASC. NASA, NASB and NASC could not be told apart.

It was also seen that re-selecting the peaks for comparison when trying to further distinguish between the twelve rolls resulted in tighter clustering of the datapoints and a better differentiation between most rolls of the same type.

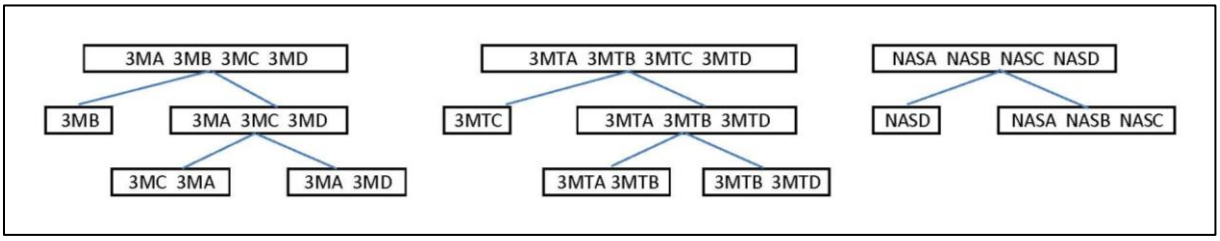

Figure 28: Summary of quantitative comparison results

Limitations of sample size

Squares of 1cm x 1cm were analyzed on a low background holder. The main effect of the smaller sample size was an increase in the noise seen. Running the smaller samples with an increased run time showed to be an effective way to compensate for the small sample size.

3MTA, 3MTB, 3MTC, 3MTD, small 3MTB

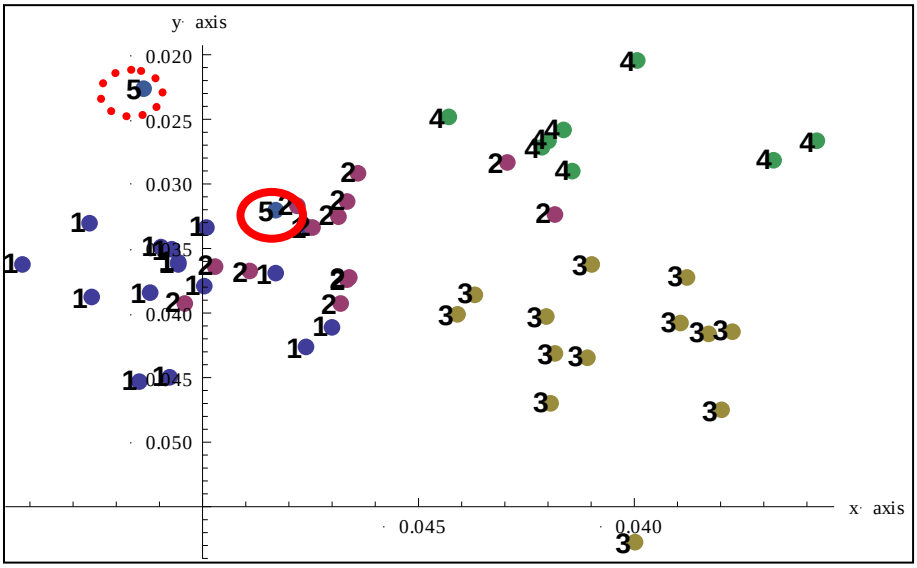

Figure 29: 2D CVA of 3MTA(1), 3MTB(2), 3MTC(3), 3MTD(4), small 3MTB(5)
Angle between the axes = 77.1

The small sample, seen above circled with a solid line, run for a longer time (scan speed 0.2) clustered close to tapes from the same roll (group 2, 3MTB), while the same small sample run for a shorter time (scan speed 1.0, which is the speed used on the

regular sized samples) seen on the top left circled by a dotted line, is quite a bit further away.

The small samples were also compared with the three types to determine if they would cluster with the 3MT tapes

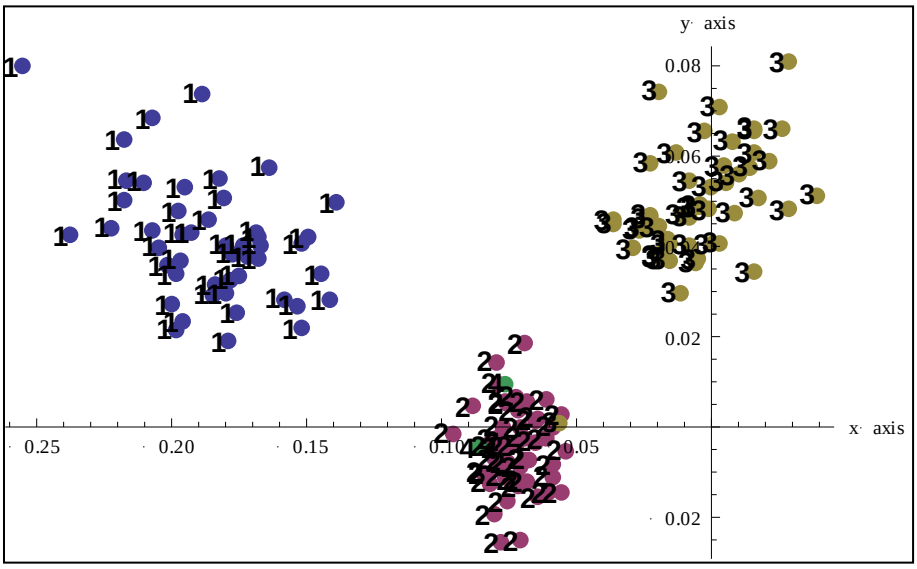

Figure 30: 2D CVA of 3M(1), 3MT(2), NAS(3), small 3MTB(4)
Angle between axes= 79.3

Although it can be hard to locate the numbers in the above schematic, both of the small 3MTB samples do cluster within the 3MT group above. This indicates that even a lower quality scan from a small sample can be useful for some discrimination between similar tapes.

Polyethylene backing

The adhesive was removed from some tapes and the backing alone was run on the low background sample holder with the spinning function disabled. The peaks found in the backing were selected from the whole tape scans and quantitative comparisons made based on those peaks alone. The peak list can be seen in Appendix C.

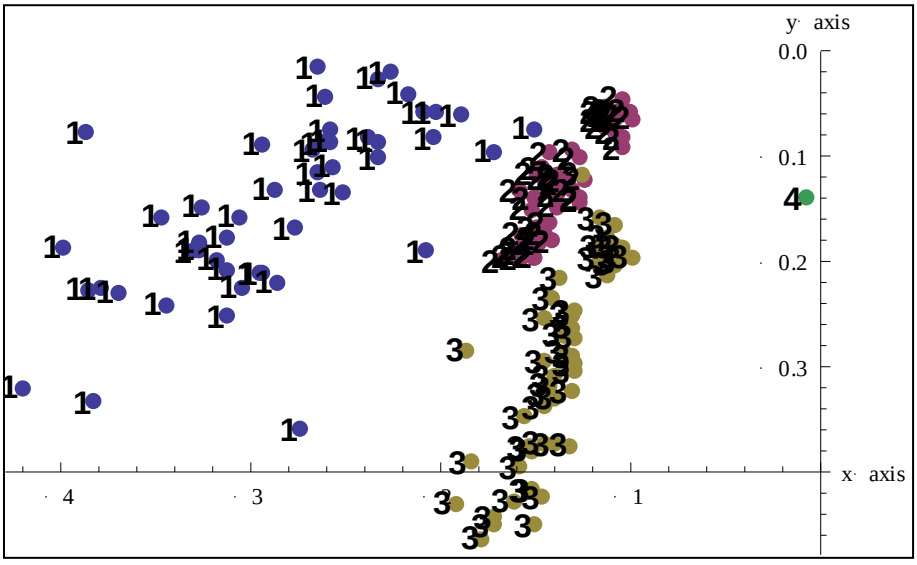

Figure 31: 2D PCA of PE peaks, 3M (1), 3MT(2), NAS(3), 3MTB backing only(4)

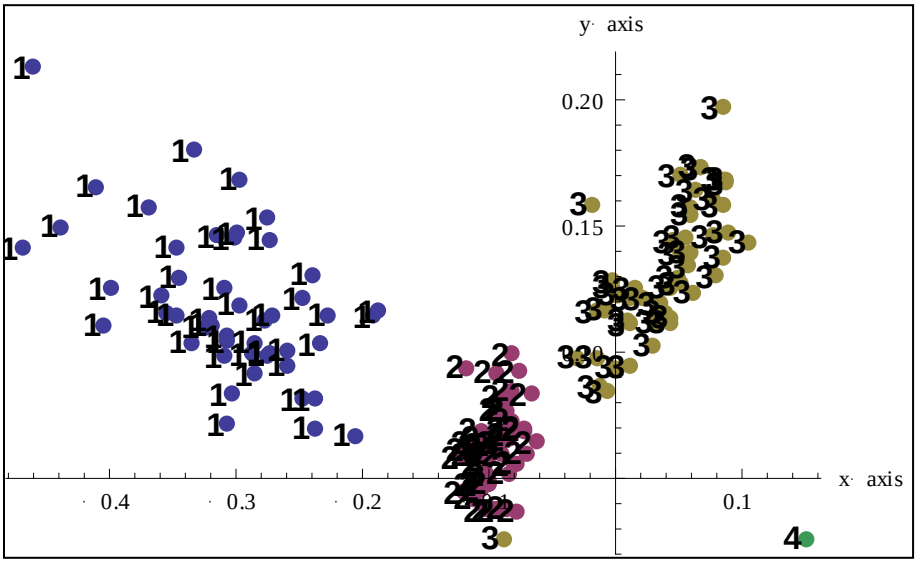

Figure 32: 2D CVA of PE peaks, 3M (1), 3MT(2), NAS(3), 3MTB backing only(4)
Angle between axes 68.9

Comparing the scan of the backing on its own with the full tapes did not result in the inclusion of the backing only scan in the correct cluster of points, despite of the selection of peaks for comparison being based on the backing. That suggests that whole and part tapes cannot be compared to each other simply by varying the selection of peaks. The backing would need to be removed from all of the tapes in order to allow for an appropriate comparison.

The distribution of datapoints in the comparison based on peaks found in the backing closely resembles that obtained using peaks from both the adhesive and the backing, suggesting that the backing does contribute to the differentiation seen. This can

be explored in further research by running a larger set of backings with the adhesive removed.

Orientation Effects

Orientation effects in the polymer backing were explored by running the backing only on a stationary sample holder with the direction of the x-rays first running along the length or the tape, and then with the x-rays running across the width of the tape.

There were no discernable differences in the diffractograms with the two orientations (see below).

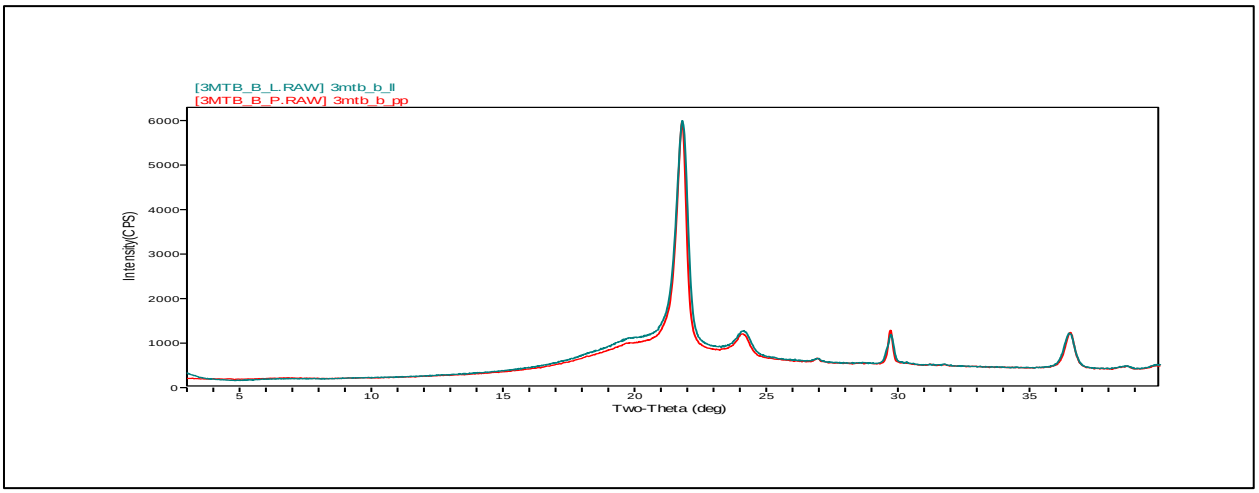

Figure 33: 3MTB, backing only, perpendicular vs parallel

This is not entirely surprising since the functional "orientation", or directionality of the properties of duct tapes is provided by the scrim rather than the polyethylene

backing. Without the scrim, the backing layer tears equally easily in both directions. Some degree of orientation effect might be observable with a transmission XRD, but this instrument was not available.

Blind Validation Study

Once appropriate instrumental parameters and statistical analysis approaches were selected using the 12 rolls mentioned above, a validation test was done using samples provided by the Chemistry Unit of the FBI laboratory.

The FBI provided 18 tape samples from 14 rolls. These 18 tape samples came from 14 rolls and included 16 grey tapes as well as two white tapes. Since the method parameters were determined using grey tapes, only the 16 grey tapes were used for the validation study.

The samples were labeled individually so that there was no indication of which ones came from the same roll. The samples were selected in order to enable comparison of the differentiation achieved by this method to that which can be achieved by routine tape examinations. The sample set contained some tapes which were from rolls that could not be told apart using routine methods and some from rolls which had similar compositions but that could be differentiated with the currently used methods.

Once the results from the qualitative XRD were sent to the FBI, the actual identity of the samples was disclosed. The routine examinations used by the FBI include

microscopical exams, FTIR, SEM/EDS, and qualitative XRD.

In the validation study, only XRD was used to distinguish between the tapes despite the fact that it would not be one of the first methods used in an actual examination protocol. Due to the lack of available expertise and time, the microscopical and FTIR examinations that are normally performed before XRD were not undertaken.

Based on an initial qualitative comparison, the 16 tapes were divided into four groups as follows:

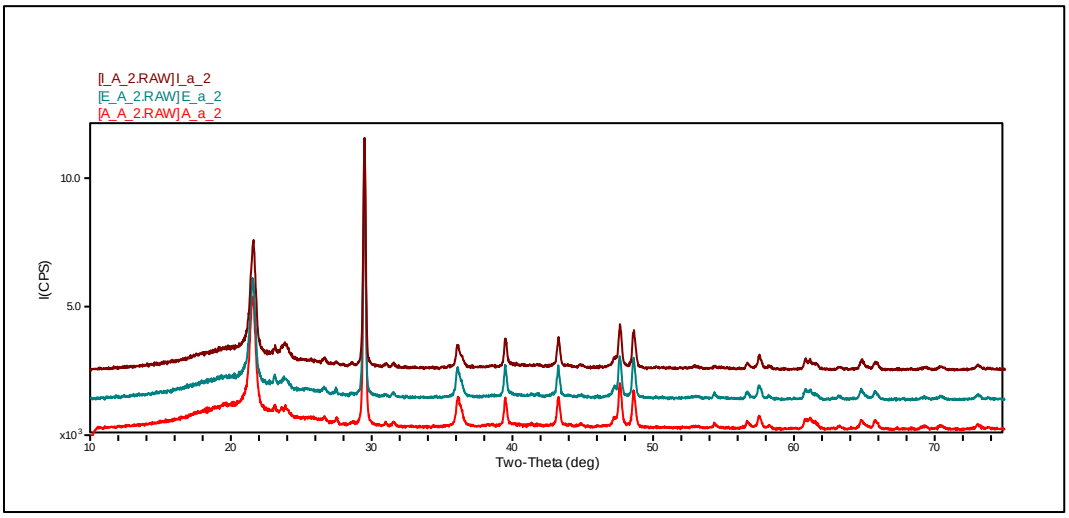

Figure 34: Group 1: A,E,I

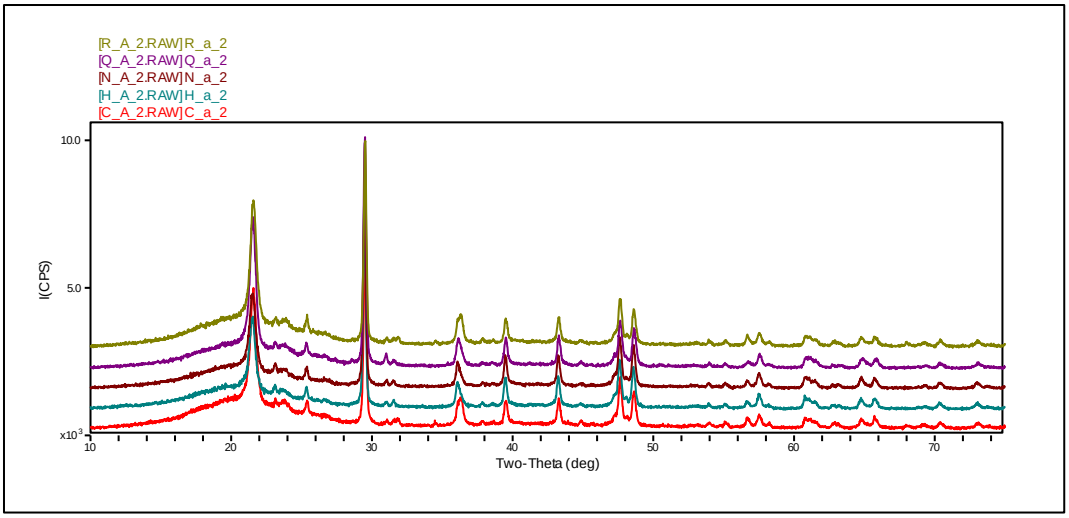

Figure 35: Group 2: C,H,N,Q,R

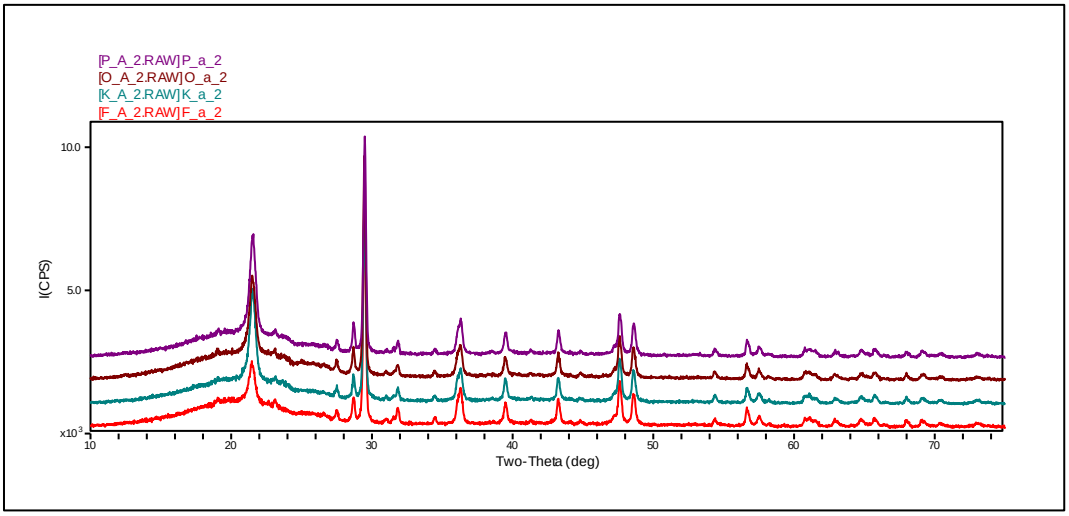

Figure 36: Group 3: F,K,O,P

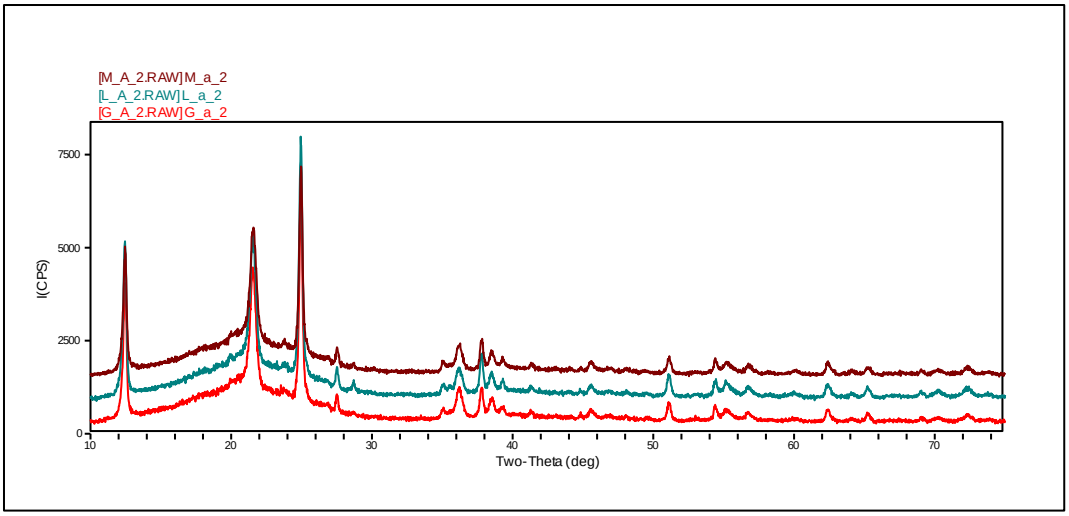

Figure 37: Group 4: G,L,M

These groups were then further examined using the quantitative comparison method. The selection of peaks to use in the comparison was done separately for each group. The peaks chosen are listed in Appendix C.

It should be remembered here that LDA and/or Hold-one-Out misclassification was only one criterion on which the decision to exclude the possibility of a common source was based. The extent to which the samples clustered (vs. being evenly spaced out) was also taken into consideration. Where the datapoints did not form obvious clusters, there was less confidence in the ability of the statistical model to create distinct groups, i.e. to distinguish between the tapes. This was particularly an issue since the number of samples was limited to five per tape.

Group 1: A, E, I

These comparisons were based on the area of 20 peaks.

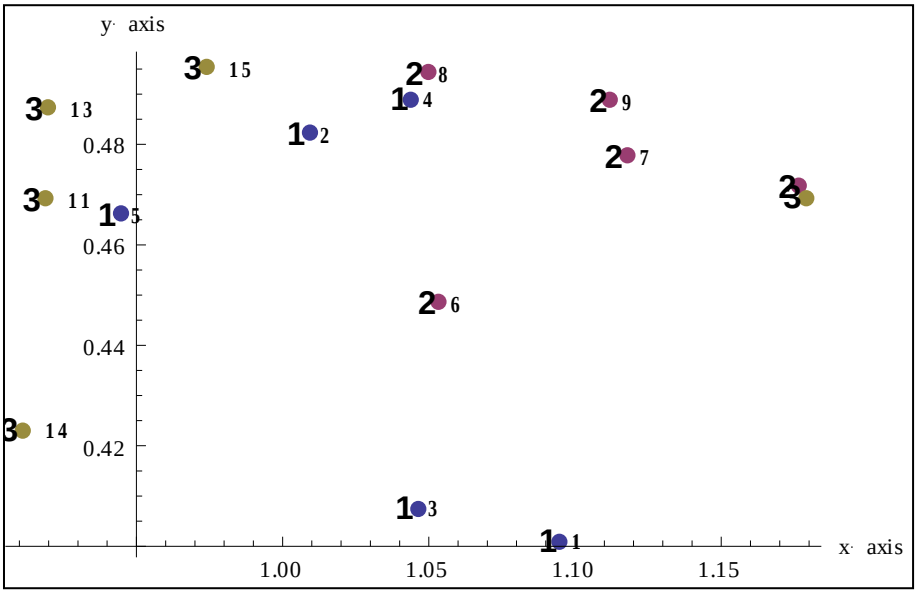

Figure 38: 2D PCA of A(1), E(2), I(3)

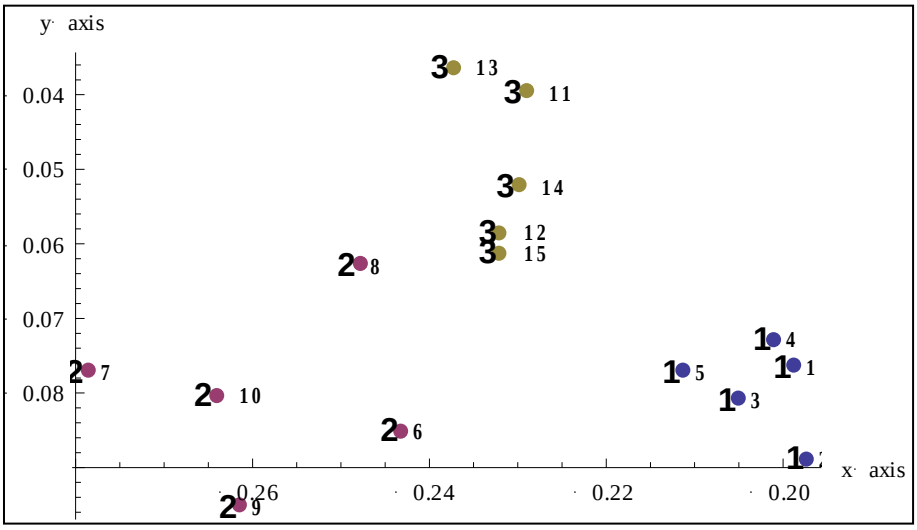

Figure 39: 2D CVA of the first 5 PCs (A,E,I)
Angle between axes 123. 1

2D CVA OF 5 PCs	A	E	I	% Misclassified
A	4		0	**0.00**
E		5	1	**20.00**
I			5	**0.00**

Table 8: Hold-one-Out of 2D CVA (A,E, I)

These all appear to cluster separately with the CVA but 2 and 3 are still quite close. Hold-one-Out verification of the CVA misclassifies sample 8 from group 2 as belonging to group 3. Based on this one can conclude that Tape A can be distinguished from tapes E and I but that E and I cannot be readily differentiated based on the available data.

These three samples came from different rolls . The only difference seen with routine examinations was that tape A has a different backing structure than the other two, which is in line with it clustering separately from E and I.

Group 2: C, H, N, Q, R

These comparisons were based on the areas of 17 peaks.

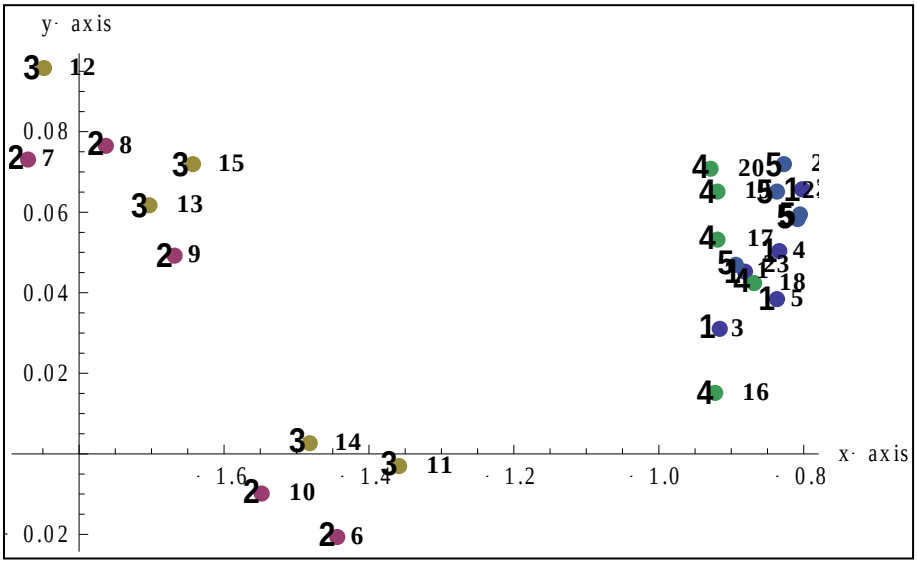

Figure 40: 2D PCA of C(1), H(2), N(3), Q(4), R(5)

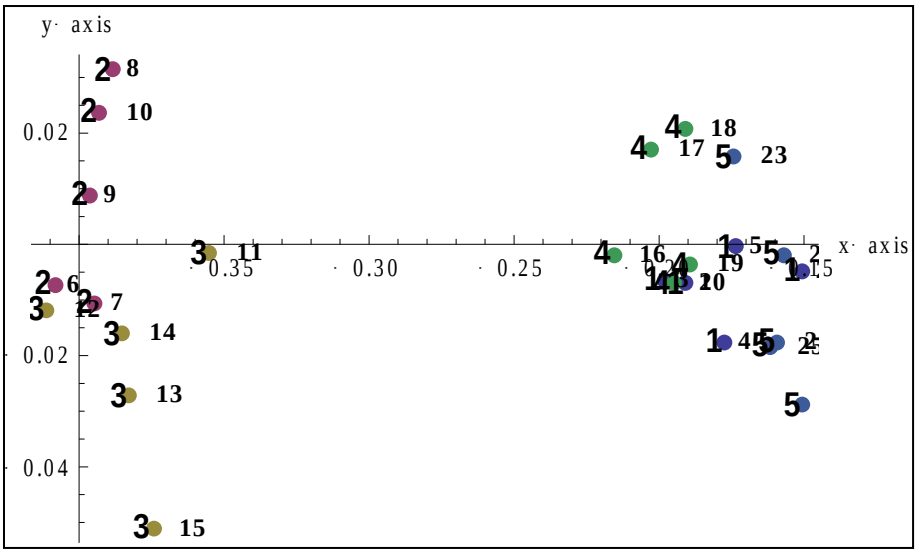

Figure 41: 2D CVA of the first five PCs (C,H, N, Q, R)
Angle between the axes 87.0

Here there appear to be two groups, H &N and C&Q&R. These two were considered separately., but still using the areas of the same 17 peaks selected for this group.

C, Q, R:

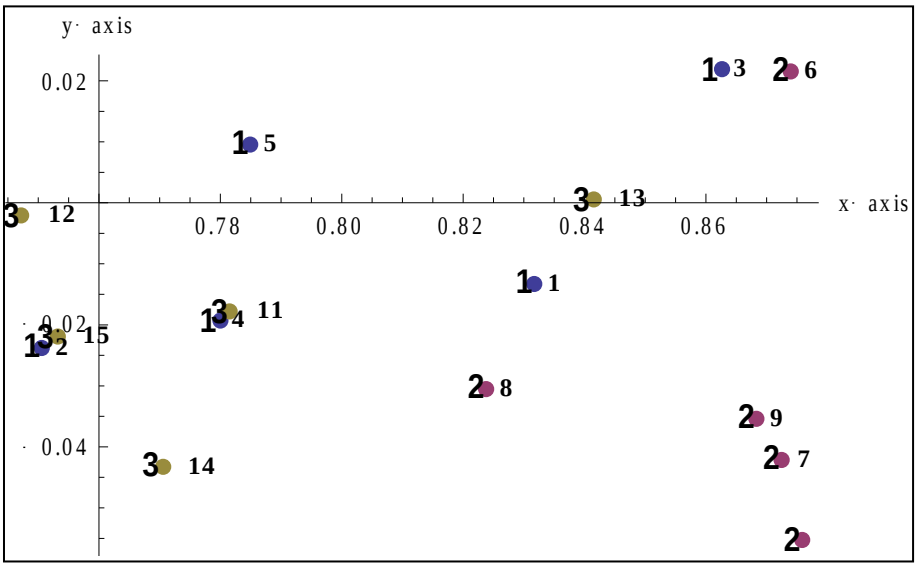

Figure 42: 2D PCA of C(1), Q(2), R(3)

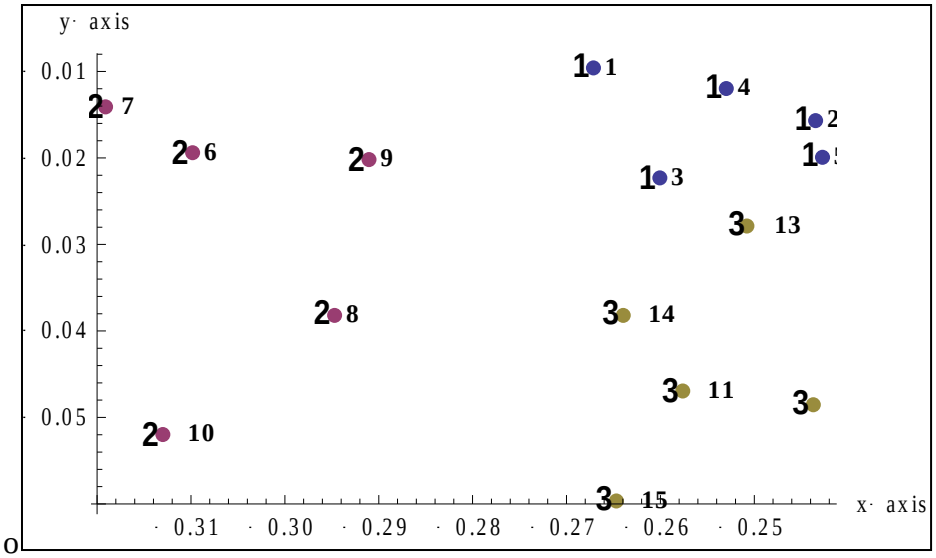

Figure 43: 2D CVA of the first five PCs (C,Q,R)
Angle between the axes 81.2

2D CVA OF 5 PCs	C	Q	R	% Misclassified
C	5			**0.00**
Q		5		**0.00**
R	1		4	**20.00**

Table 9: Hold-one-Out of 2D CVA (C, Q, R)

Here, Q is clustering away from both C and R. In both LDA and Hold-one-Out verification of the CVA results, sample 13 is misclassified as belonging to group 1.

C and R are from the same roll. Q came from another roll but was not even grouped with C and R by the routine FBI examination. C and R were grouped with J for comparison; that group was also considered and the results can be found at the end of this section.

H, N:

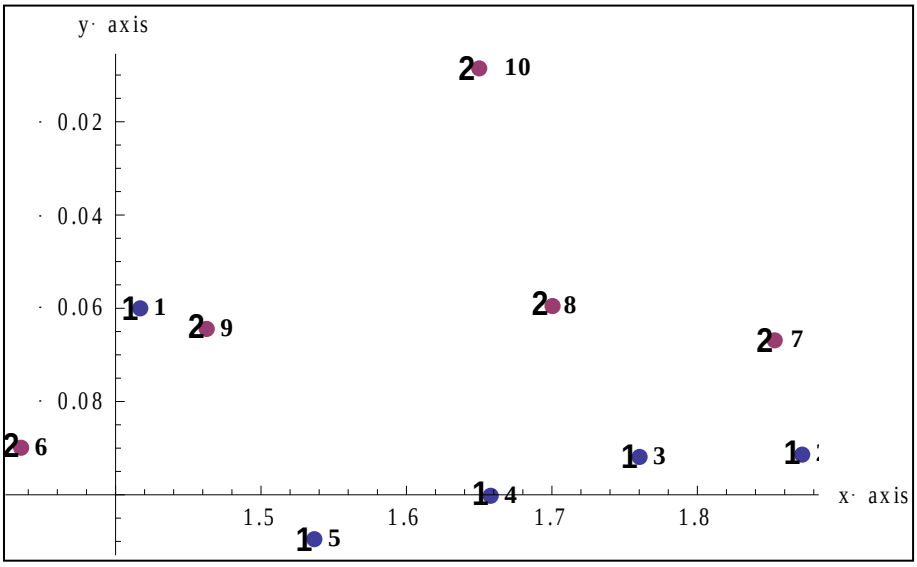

Figure 44: 2D PCA of H(1) and N(2)

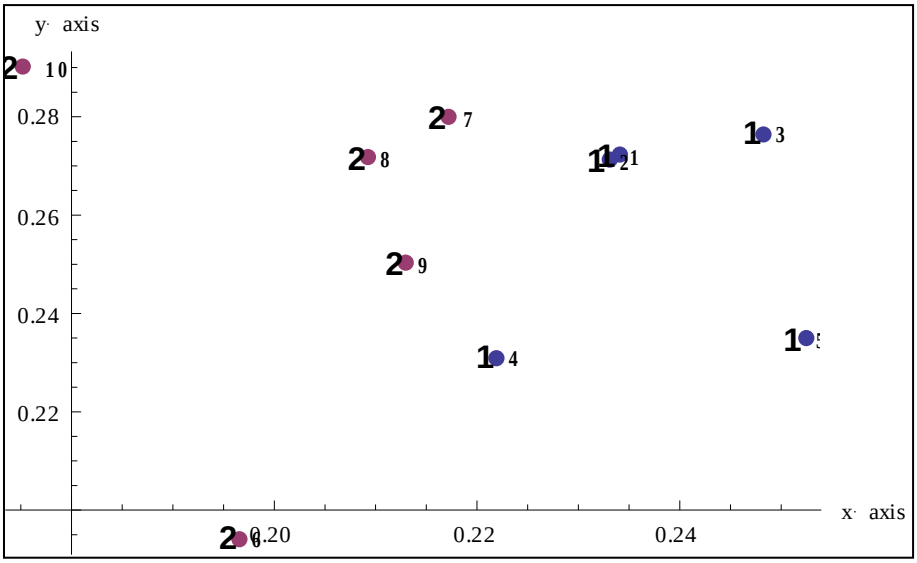

Figure 45:2D CVA of the first 5 PCs (H, N)
Angle between the axes 73.9

Though the two appear to be somewhat separated by the CVA, there is not much clustering apparent and Hold-one-Out verification of the CVA results misclassifies both 4 and 7 as belonging to the wrong group.

H and N come from the same roll. They were grouped with Q for comparison by the FBI since routine examinations were not able to distinguish between the two rolls. Even though H&N were clearly distinguished from Q in the comparison of the five members of group 2, the three were also processed as a group of their own. The results of that comparison can be seen in the end of this section. Both the Q and the H/N roll were Intertape tapes, albeit with different labels and numbers on the packaging.

Group 3: F, K, O, P

These comparisons were based on the areas of 26 peaks.

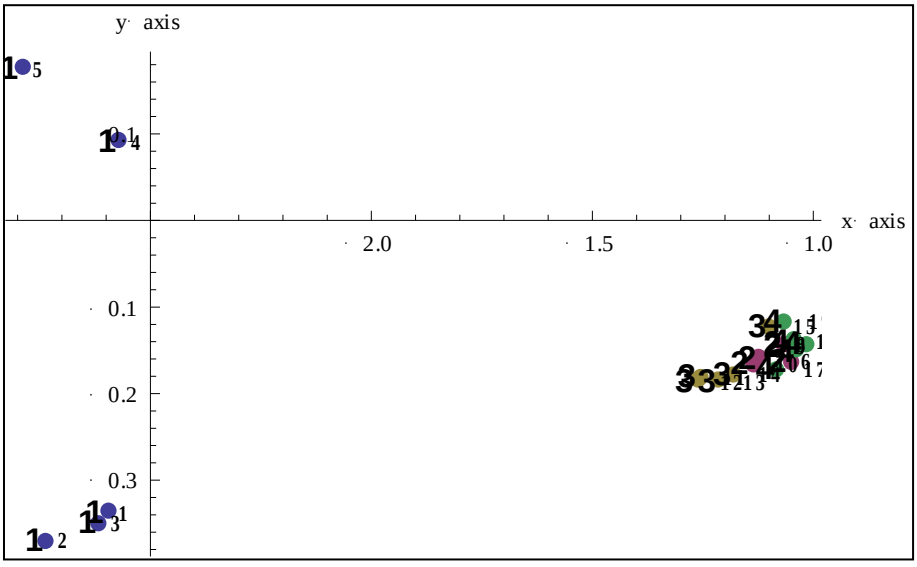

Figure 46: 2D PCA of F(1), K(2), O(3), P(4)

Since the most of the variance separated F and the other three, K, O & P were compared without F to see if they could be told apart as well.

K, O, P:

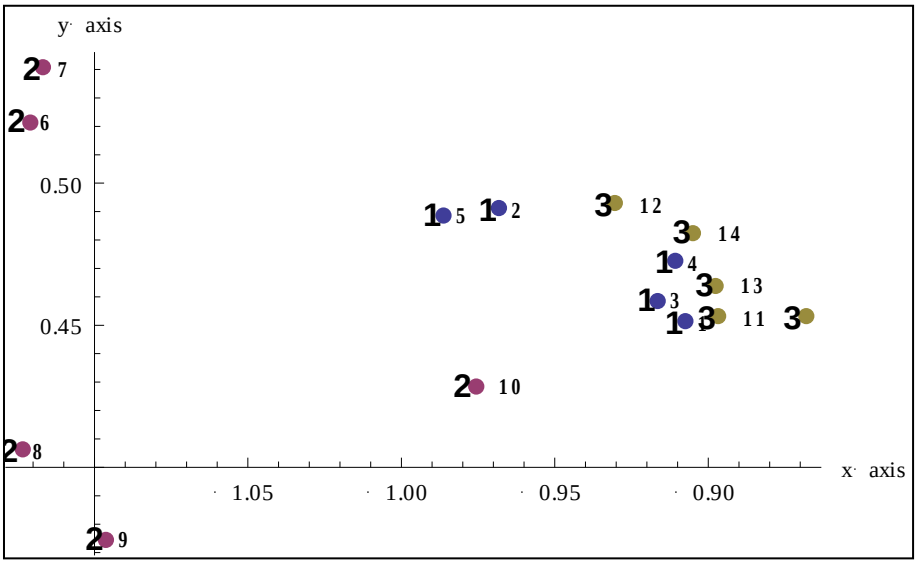

Figure 47: 2D PCA of K(1), O(2), P(3)

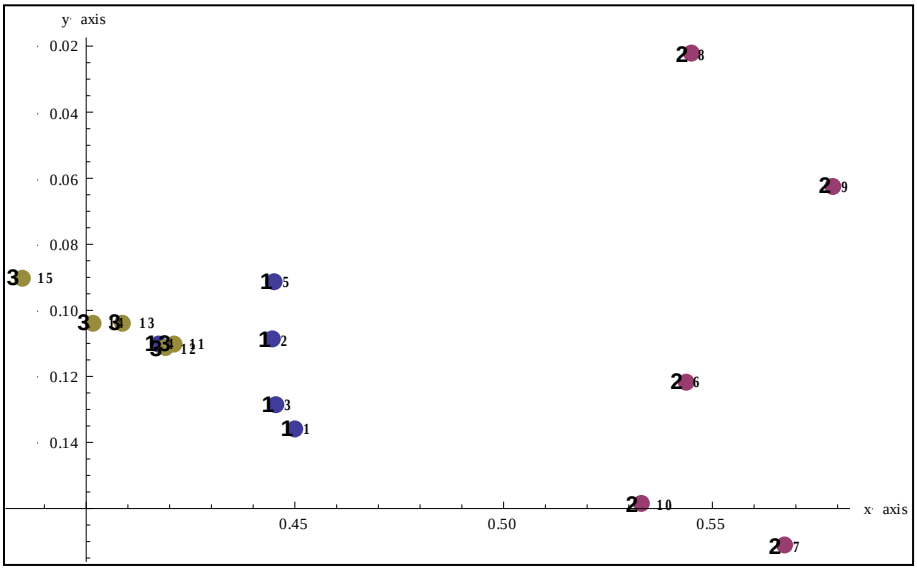

Figure 48: 2D CVA of the first 3 PCs (K,O,P)
Angle between the axes= 114.4

2D CVA OF 5 PCs	K	O	P	% Misclassified
K	4		1	**20.00**
O		5		**0.00**
P	0		5	**0.00**

Table 10: Hold-one-Out of 2D CVA (K, O, P)

Both F and O cluster away from K&P, but there is still some overlap between K&P.

Out of this set, K and P both came from the same roll. F and O were from two different rolls. All three rolls were Tesa general purpose tapes with different production codes and dates. Routine FBI examinations were unable to tell these three apart, so this was an instance in which Quantitative XRD provided added value.

Group 4: G, L, M

These comparisons were based on the areas of 20 peaks.

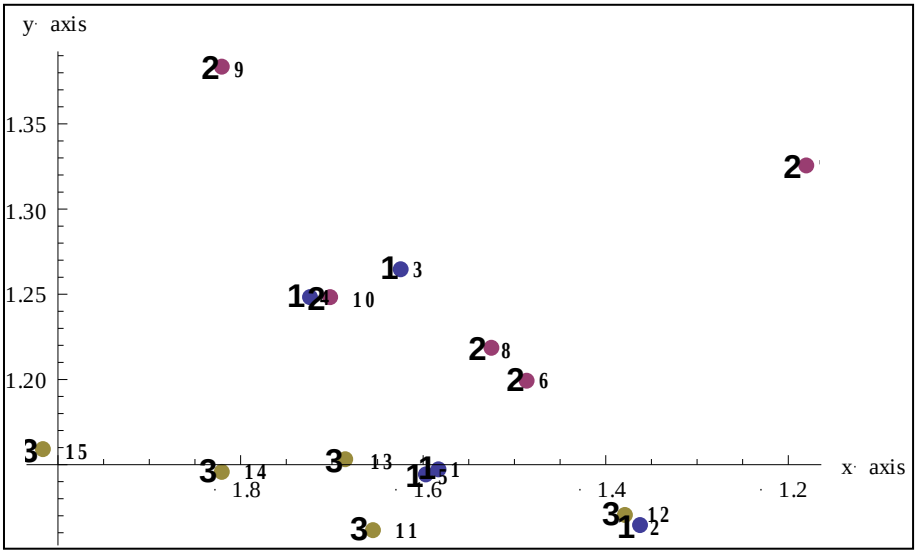

Figure 49: 2D PCA of G(1), L(2), M(3)

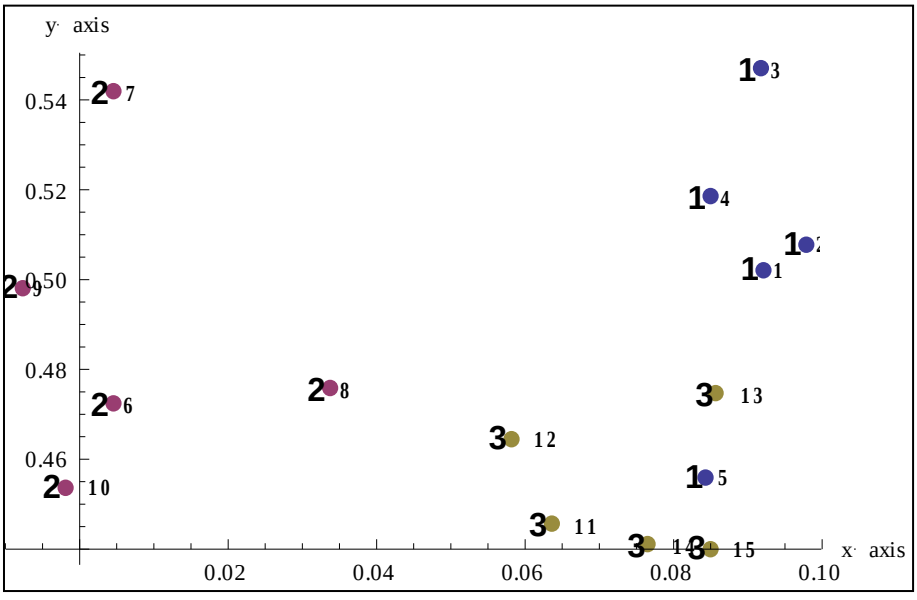

Figure 50: CVA of the first 5 PCs (G,L,M)
Angle between the axes 42.0

2D CVA OF 5 PCs	G	L	M	% Misclassified
G	4		1	**20.00**
L		5		**0.00**
M	1		4	**20.00**

Table 11: Hold-one-Out of 2D CVA (G, L, M)

G & M show quite a bit of overlap but L seems to be clustering separately. Hold-one-Out verification of the CVA misclassifies samples 5 and 13.

G and M came from the same roll while L came from a different one. These two are rolls that can be distinguished between using current FBI methods.

Other Groups of Tapes Compared

Based on comparison groups suggested by the FBI, two additional groups were also compared. H,N and Q as well as C, R and J. For these, the process was repeated from the excel peak choice onwards in order to simulate the grouping having been determined with other methods prior to the quantitative comparison.

H, N, Q

These comparisons were based on the areas of 19 peaks

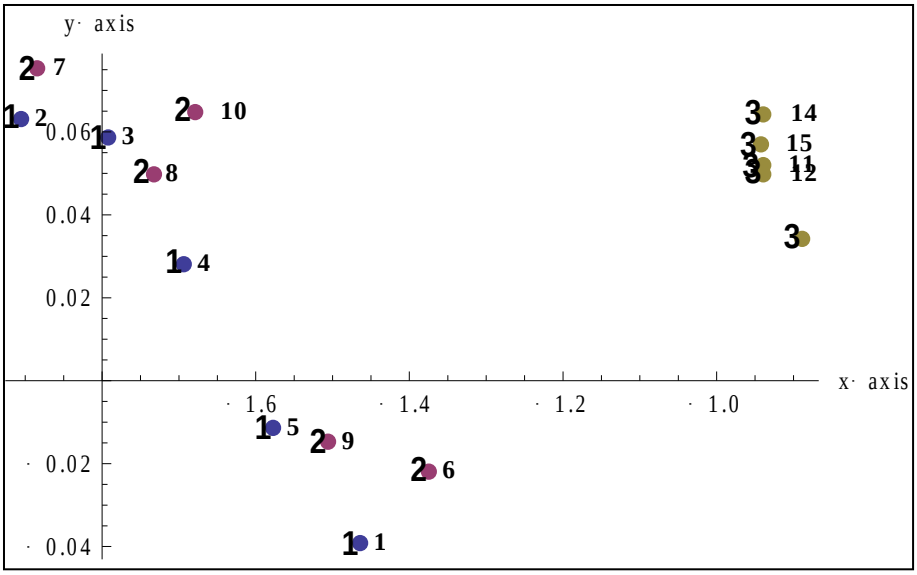

Figure 51: 2D PCA of H(1), N(2), Q(3)

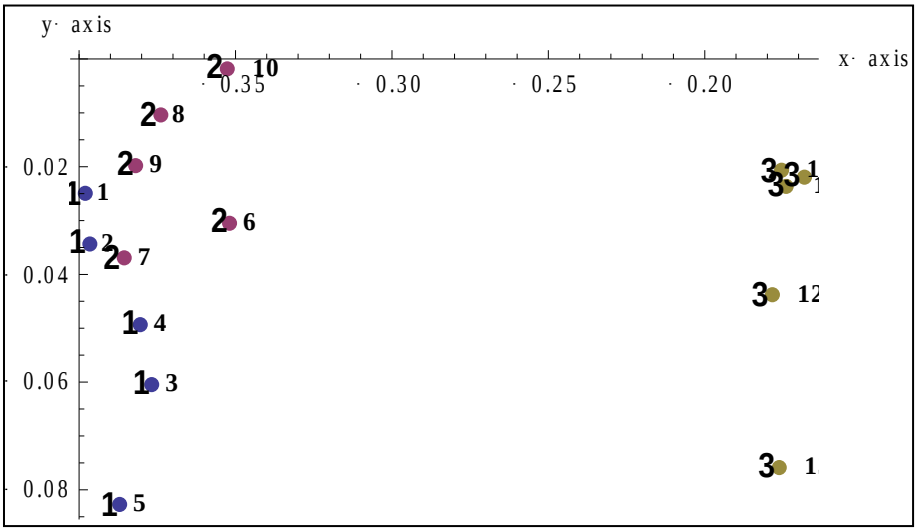

Figure 52: 2D CVA of the first 3 PCs (H,N,Q)
Angle between the axes= 90.7

2D CVA OF 3 PCs	H	N	Q	% Misclassified
H	5			**0.00**
N	1	4		**20.00**
Q			5	**0.00**

Table 12: Hold-one-Out of 2D CVA (H, N, Q)

In both of these, there is overlap between H&N while Q clusters separately. H and N came from the same roll of tape, while Q came from a different roll, one that could not be told apart from H and N using the current methods.

C, J, R

These comparisons were based on the areas of 20 peaks.

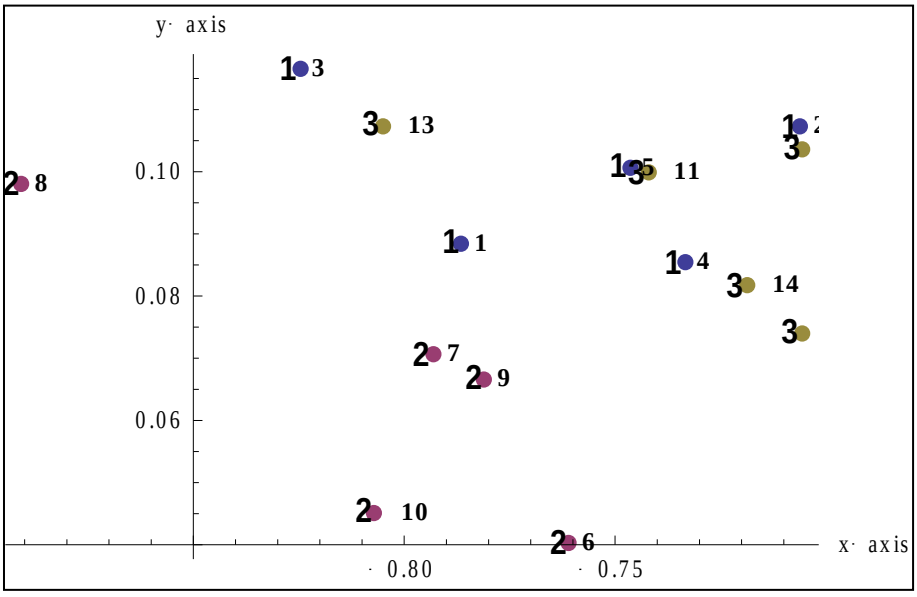

Figure 53: 2D PCA of C(1), J(2), R(3)

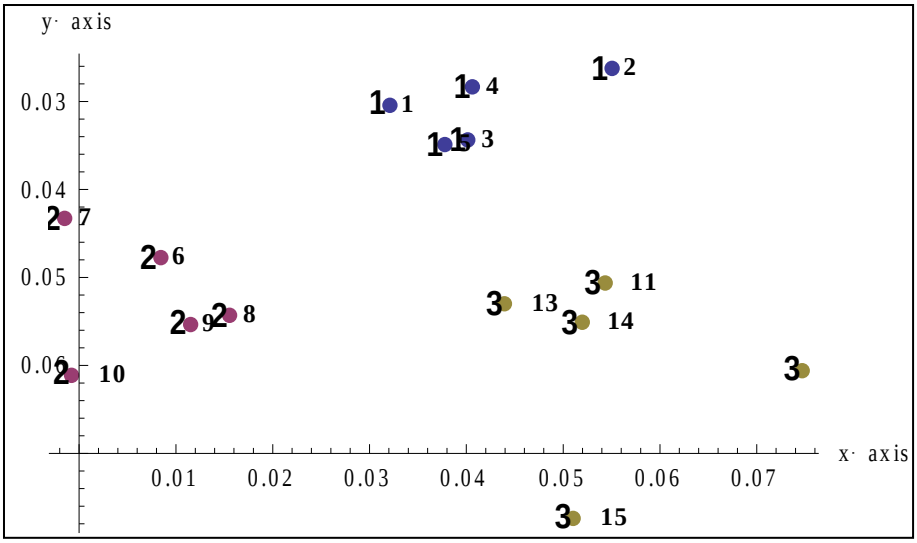

Figure 54: CVA of the first 5 PCs (C,J,R)
Angle between axes 109.5

Here all three cluster separately in the CVA though J is further away from C and R than C and R are from each other.

C and R are from the same roll, J is from a different one. The separate clustering of C and R highlights the importance of dividing the tapes into groups based on Qualitative similarity prior to undertaking the Quantitative Comparison. It also suggests that the danger of over-fitting the data is something that one should be aware of. Running more samples from each tape, and samples from a longer distance of tape, where available, in order to get a better representation of the variation present in a given roll of tape, should mitigate the over-fitting of data.

Another way of checking for over-fitting of the data is to split samples known to be from the same group into two groups (similar to where the 3M, 3MT and NAS tapes were compared both as three groups and as twelve groups). This would present them as

separate groups to the CVA model, ensuring that the clustering seen was based on differences attributable to "true" difference in the tape rolls and not the user-based group labels.

The problem seen with the separate clustering of C and R that is seen in the C, R,J comparison, is not apparent in the first comparison of C and R with H, N and Q. The number of peaks considered is actually higher in the CRJ comparison, suggesting that the problem seen is not caused by a lack of data quantity.

As can be seen below, J has an extra diffraction peak at 28.7 2θ that C and R don't have. This peak was not used for the quantitative comparison since it was not present in C and R. This suggests that it is important to base the grouping for the quantitative comparison on the qualitative XRD data, and that quantitative comparisons are most effective when the peaks chosen are specific to the samples being compared, as opposed to a selection of peaks used for all samples.

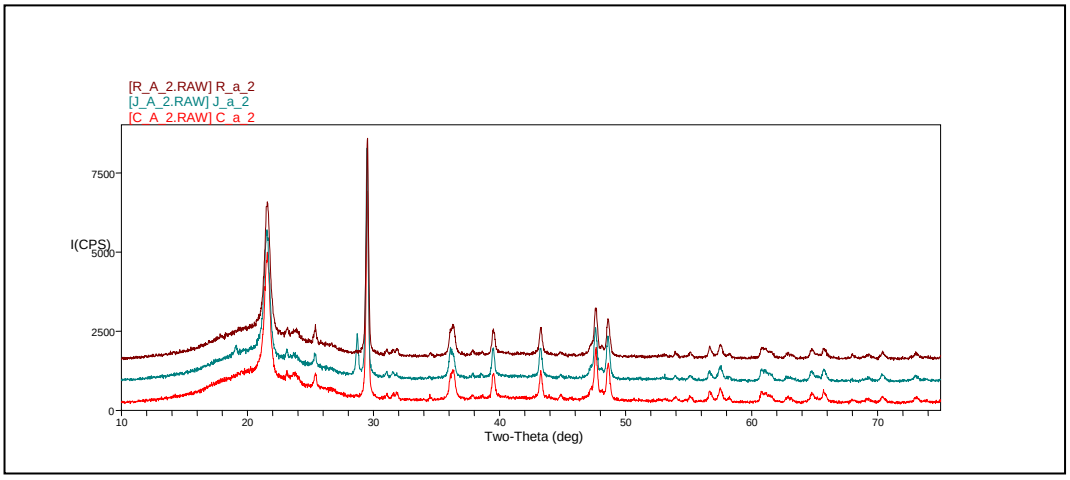

Figure 55: Qualitative comparison of C,J,R

Blind Validation Study Conclusions:

This validation study showed that adding a quantitative comparison of the x-ray diffraction peak areas resulted in an increased ability to distinguish between similar duct tapes that came from different rolls in some instances.

In the case of Group 1 (A,E,I), quantitative XRD comparison achieved the same level of discrimination as routine methods. In the cases of group 2 (C, H, N, Q, R) and 3 (F, K, O, P), quantitative XRD was able to differentiate between tapes known to come from separate rolls but not distinguishable by routine methods. This suggests that quantitative XRD comparison best fits into the examination process after microscopical examinations, FTIR, SEM/EDX and qualitative XRD. The results of quantitatively comparing C, R and J despite their qualitative XRD differences highlights the importance of qualitative comparison prior to quantitative comparison.

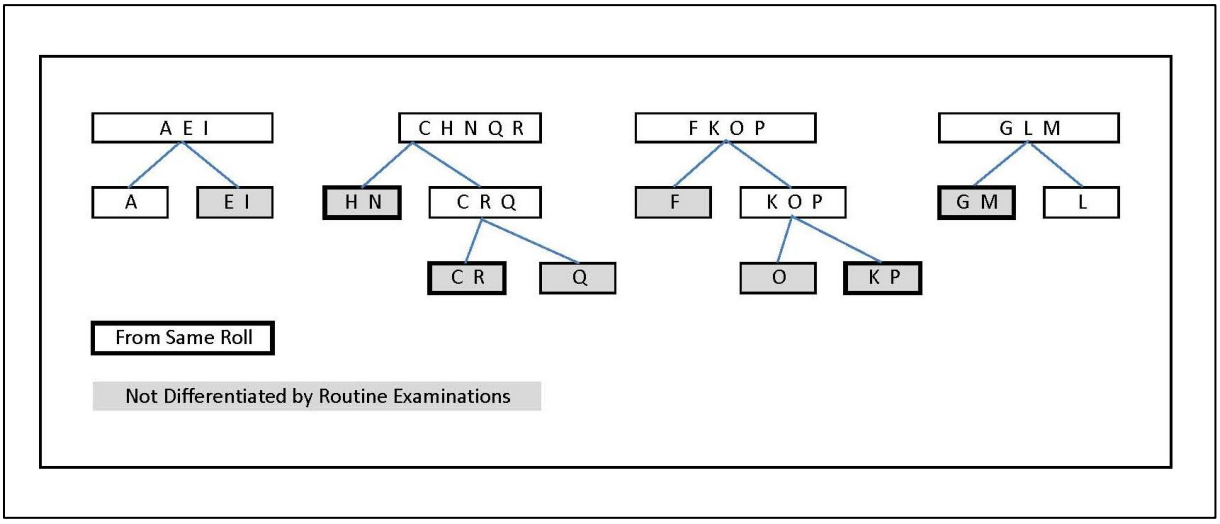

Figure 56: Summary of Blind Verification Results

V. General Conclusions

Summary of results and recommended analysis scheme

These results have shown that a quantitative comparison using statistical methods can further distinguish between some tapes whose diffractograms are qualitatively indistinguishable, and which cannot be told apart using current techniques .

Tapes from different brands were told apart using statistical comparisons even where their diffractograms were very similar. However, on several occasions, the difference between rolls from the same brand was not sufficient to be able to tell them apart.

This indicates that the main use of the quantitative XRD comparison is one of exclusion. This means that where datapoints are seen to cluster separately, one can exclude the possibility of the samples coming from the same roll. However, the absence of such clustering should not be interpreted as evidence of the samples originating from the same roll. Also, as was seen in the blind validation study, the choice of samples which are inter-compared and selection of peaks used in the comparison can have a severe effect on the outcome of the quantitative comparison.

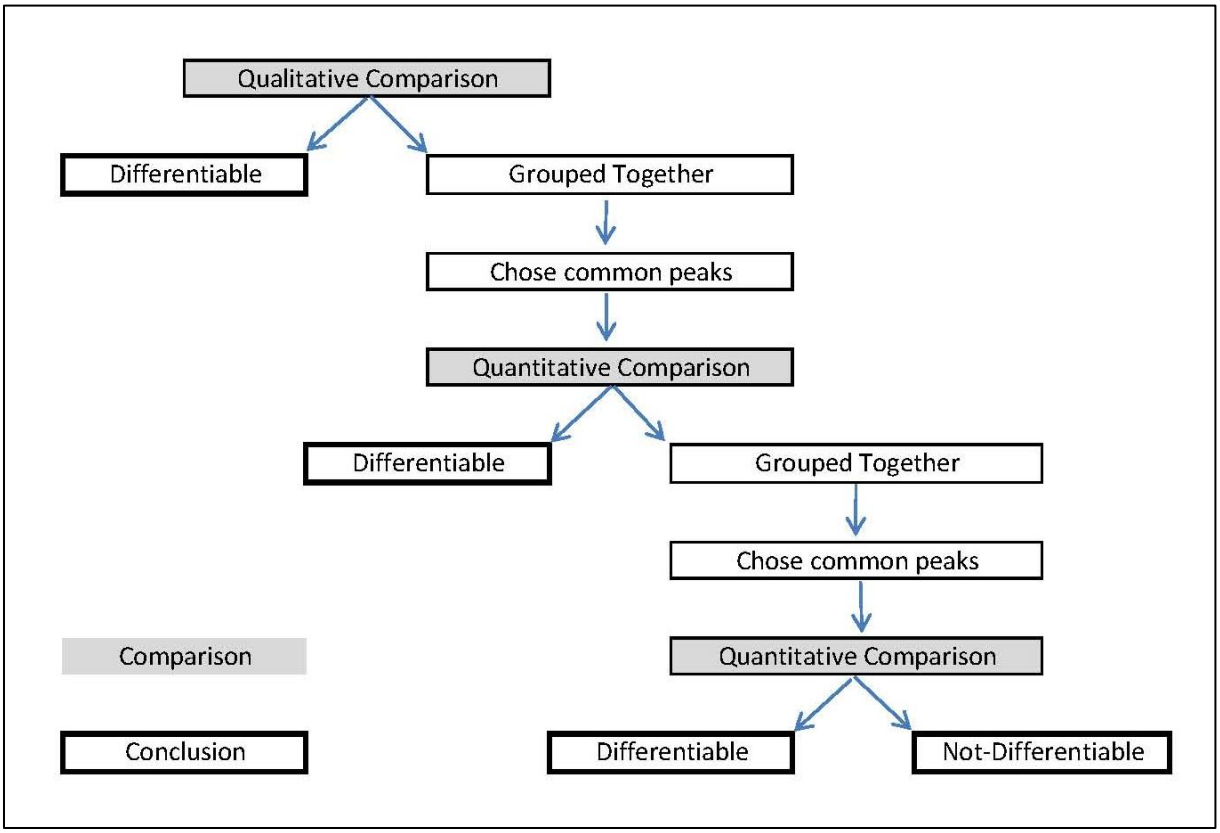

Figure 57: Recommended XRD Comparison Scheme

Implications for policy and practice

Comparing duct tape samples based on their composition can never hope to achieve the same level of differentiation as the more discriminate forensic samples such as fingerprints and DNA. The examination of duct tapes can nevertheless provide an investigation with useful information and provide a useful variable to include in efforts to find patterns within volume crime, for example in linking drug packaging to common sources or identifying crime series.

The results of the blind verification study seem to indicate that XRD analysis might be a viable alternative and/or addition to the current combination of methods used.

The discrimination achieved based solely on qualitative and quantitative XRD analysis, as done in the blind verification study, yielded results that were at the minimum comparable to the results obtained with traditional methods. This suggests that employing XRD analysis earlier on in the examination process might be a more time and cost effective option. Further experimentation using samples from a larger number of tape rolls should be done in order to further explore this notion.

In many cases, the results obtained using quantitative XRD were found to be more discriminatory than the current methods. In a case scenario where duct tape evidence is of importance in supporting or refuting a link, this could translate to the elimination of an suspect or line of enquiry that would not otherwise have been made.

Future Research

Further research on the use of XRD to examine duct tapes could be done using more advanced XRD instrumentation and more samples. The backing layer could be examined in more detail, by running backing samples without adhesive in both transmission and reflection mode XRD and examining orientation and crystallinity effects in the polymer. Although the advanced instrumentation required for this will most likely not be made available for routine forensic analyses in the near future, it would contribute to further explaining the results obtained with the more common desktop

XRD. The number and type of samples used in this project was limited, as the purpose was to determine the usefulness of the method rather than to conduct a population study type experiment. Looking at more rolls and types of tape would provide a valuable addition to this research. Examining tapes obtained directly from the manufacturers with knowledge of the source and production relationships between samples would help to further define the limitations of this method.

This research was conducted using tapes that were stored in a dry, dark laboratory environment. Determining how exposure to a variety of other environmental conditions affects the diffraction pattern obtained from duct tapes would be a valuable addition to this research and necessary for the application of this method to degraded and weathered samples.

Given the results seen, it might also be useful to extend research on this method to other PSA tape types.

VII. Appendices

Appendix A Sample Information

Samples run and the height compensation used to line up the diffractograms.

3M:

	Run	Δ	Run	Δ	Run	Δ	Run	Δ
1	3MA_L1	-0.4	3MB_L1	-0.41	3MC_L1	-0.42	3MD_SS1	-1.07
2	3MA_L2	-0.4	3MB_L2	-0.41	3MC_L2	-0.405	3MD1_SS1	-1.01
3	3MA_L3	-0.39	3MB_L3	-0.38	3MC_L3	-0.39	3MD2_SS1	-1.01
4	3MA1_S1	-0.4	3MB1_L1	-0.42	3MC1_S1	-0.415	3MD3_SS1	-1.025
5	3MA1_S2	-0.4	3MB1_S1	-0.42	3MC2_S1	-1.03	3MD4_SS1	0
6	3MA1_S3	-0.97	3MB2_S1	-1.03	3MC4_S1	-1.02	3MD5_SS1	0
7	3MA1_S4	-0.95	3MB3_S1	-1.02	3MC5_S1	-1.025	3MD6_SS1	0
8	3MA2_S1	-1.02	3MB4_S1	-1.085	3MC6_S1	-1.13	3MD7_SS1	0
9	3MA3_S1	-1	3MB5_S1	-1.12	3MC7_S1	-1.26		
10	3MA4_S1	-1.01	3MB6_S1	-1.15	3MC8_S1	-1.3		
11	3MA5_S1	-1.12	3MB7_S1	-1.24	3MC9_SS1	-1.185		
12	3MA6_S1	-1.13	3MB8_S1	-1.22	3MC10_SS1	-1.025		
13	3MA7_S1	-1.22	3MB9_SS1	-1.35				
14	3MA7_S2	-1.26	3MB10_SS1	-1.02				
15	3MA8_S1	-1.24						
16	3MA9_SS1	-1.32						
17	3MA10_SS1	-1.01						

3MT:

	Run	Δ	Run	Δ	Run	Δ	Run	Δ
1	3MTA_L1	-0.37	3MTB_L1	-0.37	3MTC_L1	-0.38	3MTD_SS1	-1.06
2	3MTA_L2	-0.365	3MTB_L2	-0.37	3MTC_L2	-0.38	3MTD1_SS1	-1
3	3MTA_L3	-0.36	3MTB_L3	-0.37	3MTC_L3	-0.38	3MTD2_SS1	-1
4	3MTA_S1	-0.97	3MTB1_S1	-0.38	3MTC1_S1	-0.385	3MTD3_SS1	-1
5	3MTA_S2	-0.97	3MTB2_S1	-1	3MTC2_S1	-1	3MTD4_SS1	0
6	3MTA1_S1	-0.375	3MTB3_S1	-1	3MTC3_S1	-0.995	3MTD5_SS1	0
7	3MTA1_LS1	-0.98	3MTB4_S1	-0.99	3MTC4_S1	-0.99	3MTD6_SS1	0
8	3MTA2_S1	-0.98	3MTB5_S1	-1.08	3MTC5_S1	-1.09	3MTD7_SS1	0
9	3MTA3_S1	-0.98	3MTB6_S1	-1.14	3MTC6_S1	-1.08		
10	3MTA4_S1	-1.02	3MTB7_S1	-1.23	3MTC7_S1	-1.25		
11	3MTA5_S1	-1.095	3MTB8_S1	-1.3	3MTC8_S1	-1.31		
12	3MTA6_S1	-1.07	3MTB9_S1	0	3MTC9_SS1	-1.16		
13	3MTA7_S1	-1.075	3MTB9_SS1	-1.315	3MTC10_SS1	-1.085		
14	3MTA8_S1	-1.29	3MTB10_SS1	-1.07				
15	3MTA9_SS1	-1.16	3MTB10m_L1	0.01				
16	3MTA10_SS1	-1.03	3MTB10m_S1	0.01				
17	3MTA10m_S1	-0.04						

NAS:

	Run	Δ	Run	Δ	Run	Δ	Run	Δ
1	NASA_L1	-0.365	NASB_L1	-0.36	NASC_L1	-0.355	NASD_SS1	0.96
2	NASA_L2	-0.35	NASB_L2	-0.34	NASC_L2	-0.33	NASD1_SS1	0.985
3	NASA_L3	-0.33	NASB_L3	-0.35	NASC_L3	-0.32	NASD2_SS1	-1
4	NASA1_S1	-0.39	NASB1_S1	-0.39	NASC1_S1	-0.38	NASD3_SS1	0.995
5	NASA2_S1	-0.975	NASB1_S2	-0.98	NASC2_S1	-0.99	NASD4_SS1	0
6	NASA3_S1	-0.99	NASB2_S1	-0.99	NASC3_S1	-0.965	NASD5_SS1	0
7	NASA4_S1	-1.06	NASB2_S2	-0.94	NASC4_S1	-0.98	NASD6_SS1	0
8	NASA5_S1	-1.05	NASB3_S1	-0.99	NASC5_S1	-1.07	NASD7_SS1	0
9	NASA6_S1	-1.14	NASB4_S1	-1.03	NASC6_S1	-1.09		
10	NASA7_S1	-1.08	NASB5_S1	-1.07	NASC7_S1	-1.18		
11	NASA7_S2	-1.25	NASB6_S1	-1.16	NASC7_S2	-1.1		
12	NASA8_S1	-1.225	NASB7_S1	-1.115	NASC8_S1	-1.16		
13	NASA9_SS1	-1.23	NASB7_S2	-1.255	NASC9_SS1	-1.16		
14	NASA10_SS1	-0.99	NASB8_S1	-1.16	NASC10_SS1	-0.975		
15			NASB9_SS1	-1.16				
16			NASB10_SS1	-0.99				

Distances between the Samples on the tape rolls(in mm):

3M Regular:

3MA	3MB	3MC	3MD
3MA	3MB	3MC	3MD
10	10	3MC1	824
3MA1	3MB1	110.5	3MD1
110	110.5	3MC2	3MD2
3MA2	3MB2	111	3MD3
109.5	109.5	3MC3	204
3MA3	3MB3	220	3MD4
221	220	3MC4	405
3MA4	3MB4	113	3MD5
111	118	3MC5	208
3MA5	3MB5	204	3MD6
207	206	3MC6	3MD7
3MA6	3MB6	418	
413	413	3MC7	
3MA7	3MB7	411	
415	405	3MC8	
3MA8	3MB8	3MC9	
3MA9	3MB9	3MC10	
3MA10	3MB10		

3M Tough:

3MTA	3MTB	3MTC	3MTD
3MTA	3MTB	3MTC	3MTD
3MTA1	3MTB1	3MTC1	826
112	111	115.5	3MTD1
3MTA2	3MTB2	3MTC2	3MTD2
111.5	111	89	3MTD3
3MTA3	3MTB3	3MTC3	204
220	221	220.5	3MTD4
3MTA4	3MTB4	3MTC4	413
120	128	124	3MTD5
3MTA5	3MTB5	3MTC5	205
207	209	206	3MTD6
3MTA6	3MTB6	3MTC6	3MTD7
406	413	413	
3MTA7	3MTB7	3MTC7	
409	409	417	
3MTA8	3MTB8	3MTC8	
3MTA9	3MTB9	3MTC9	
3MTA10	3MTB10	3MTC10	

Nashua:

NASA	NASB	NASC	NASD
NASA	NASB	NASC	NASD
NASA1	NASB1	NASC1	828
110	110	112	NASD1
NASA2	NASB2	NASC2	NASD2
111	110.5	110	NASD3
NASA3	NASB3	NASC3	204
222	110	221	NASD4
NASA4	NASB4	NASC4	407
144	222.5	123	NASD5
NASA5	NASB5	NASC5	208
210	203	207	NASD6
NASA6	NASB6	NASC6	NASD7
404	410	412	
NASA7	NASB7	NASC7	
411	412	409	
NASA8	NASB8	NASC8	
NASA9	NASB9	NASC9	
NASA10	NASB10	NASC10	

Appendix B Within-roll Variation & Outliers

3MA:

```
{1.25824,        72.6242,          72.6242},
{0.438431,       25.3056,          97.9298},
{0.0266138,      1.53611,          99.4659},
{0.00375932,     0.216983,         99.6829},
{0.00186924,     0.10789,          99.7908},
{0.00128325,     0.0740673,        99.8649},
```

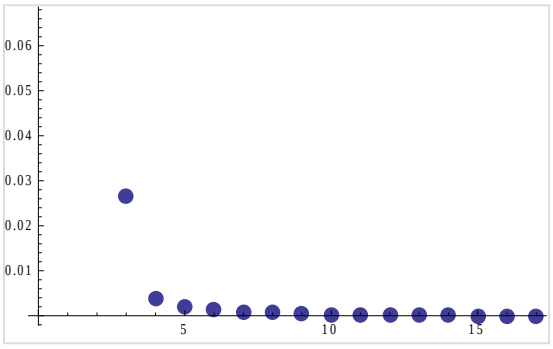

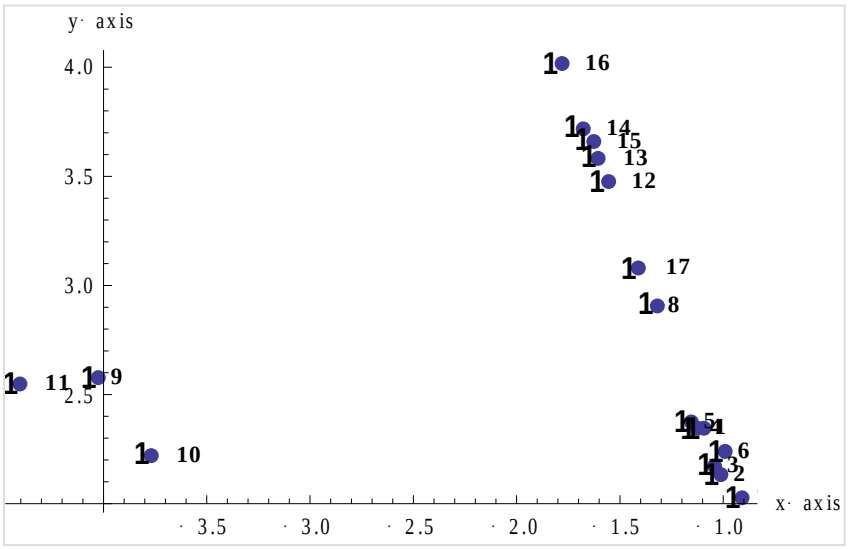

3MA_c

```
{0.589104, 93.2228, 93.2228},
{0.0330042, 5.22276, 98.4456},
{0.00445049, 0.704268, 99.1499},
{0.00147564, 0.233513, 99.3834},
{0.00133311, 0.210959, 99.5943},
{0.000993273, 0.157181, 99.7515},
```

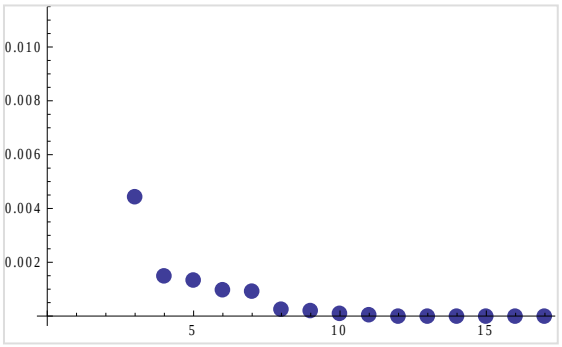

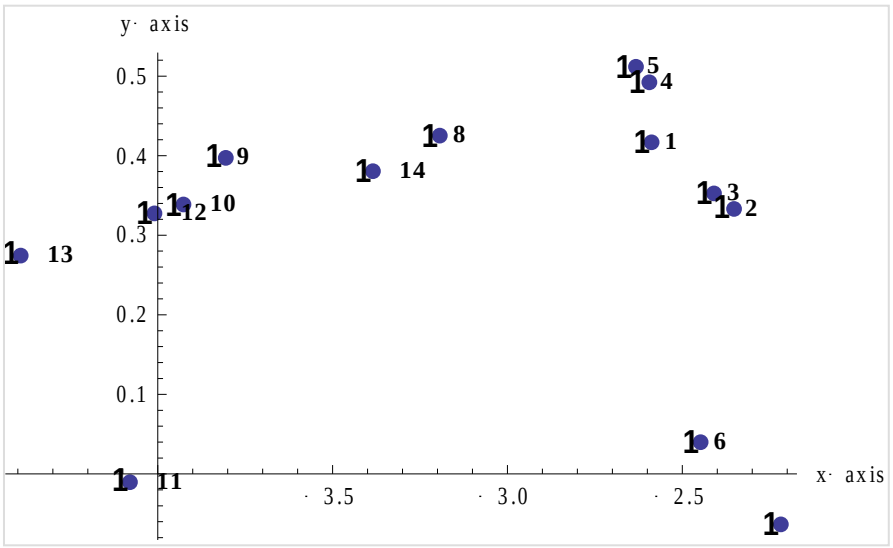

3MB

```
{0.347218,        96.7579,          96.7579},
{0.00598422,      1.6676,           98.4255},
{0.00198574,      0.553357,         98.9789},
{0.00144894,      0.403769,         99.3827},
{0.000959238,     0.267307,         99.65},
{0.000507525,     0.14143,          99.7914},
```

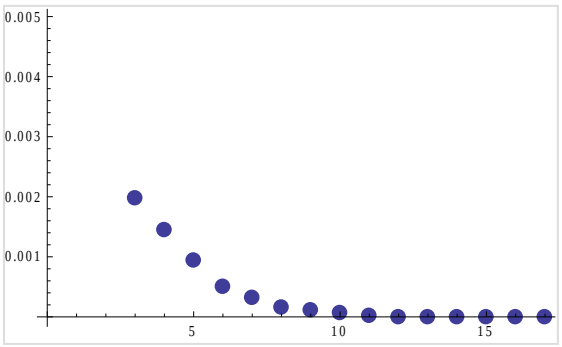

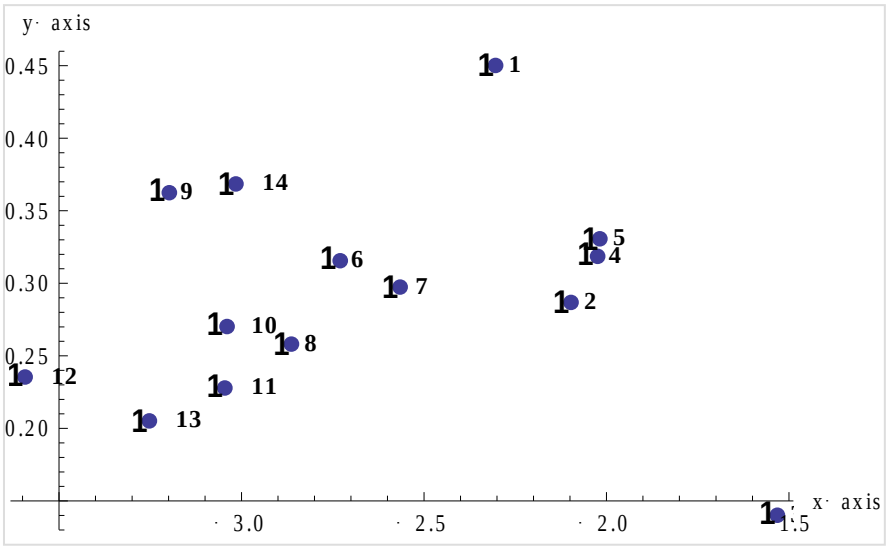

3MC

```
{0.280183,        96.2309,          96.2309},
{0.00543695,      1.86736,          98.0983},
{0.00209271,      0.718756,         98.817},
{0.00155174,      0.532956,         99.35},
{0.000762012,     0.261719,         99.6117},
{0.000502028,     0.172425,         99.7841},
```

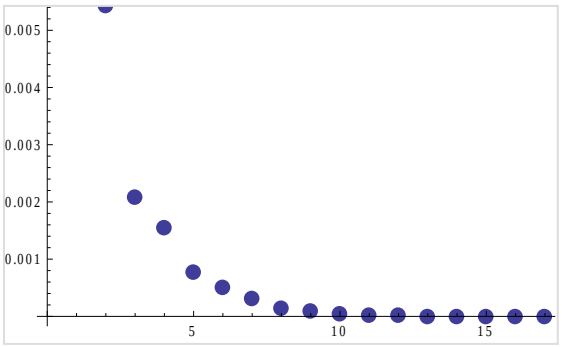

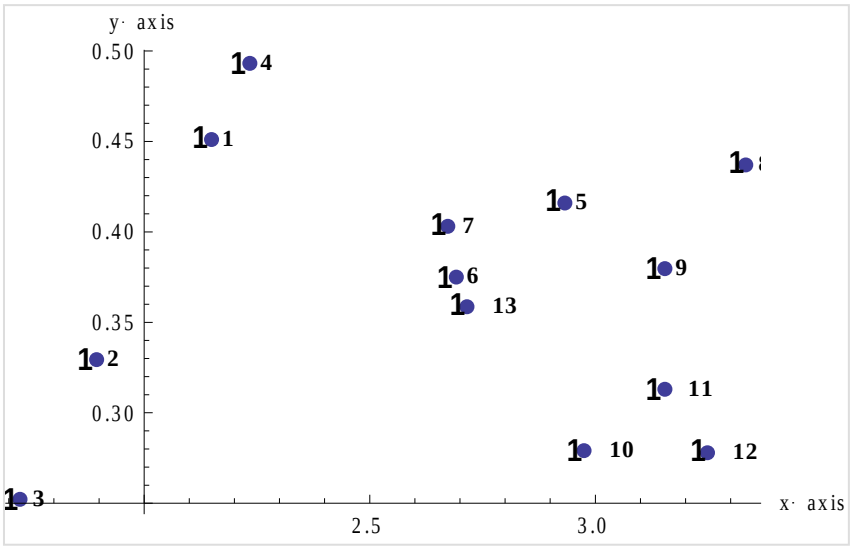

3MD

```
{0.141238,        85.8738,        85.8738},
{0.0188851,       11.4823,        97.356},
{0.00221206,      1.34495,        98.701},
{0.000862387,     0.524337,       99.2253},
{0.000629563,     0.382778,       99.6081},
{0.000437914,     0.266255,       99.8744},
```

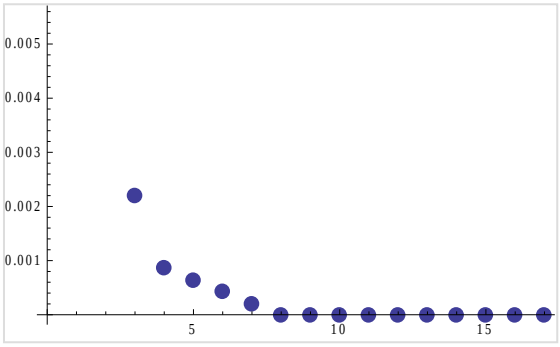

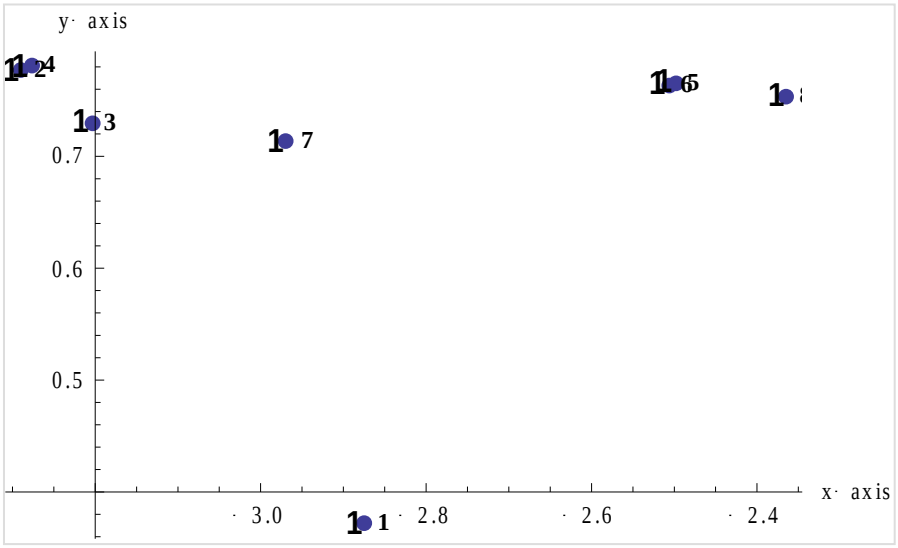

3MD_c

```
{0.164778,        96.6905,          96.6905},
{0.00295212,      1.73229,          98.4228},
{0.00110086,      0.645977,         99.0688},
{0.000765223,     0.449028,         99.5178},
{0.000533317,     0.312947,         99.8308},
{0.000288423,     0.169244,         100.},
```

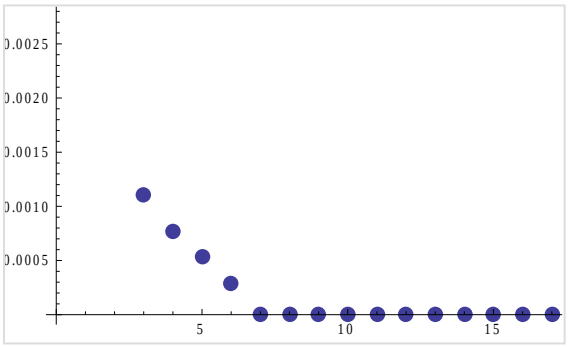

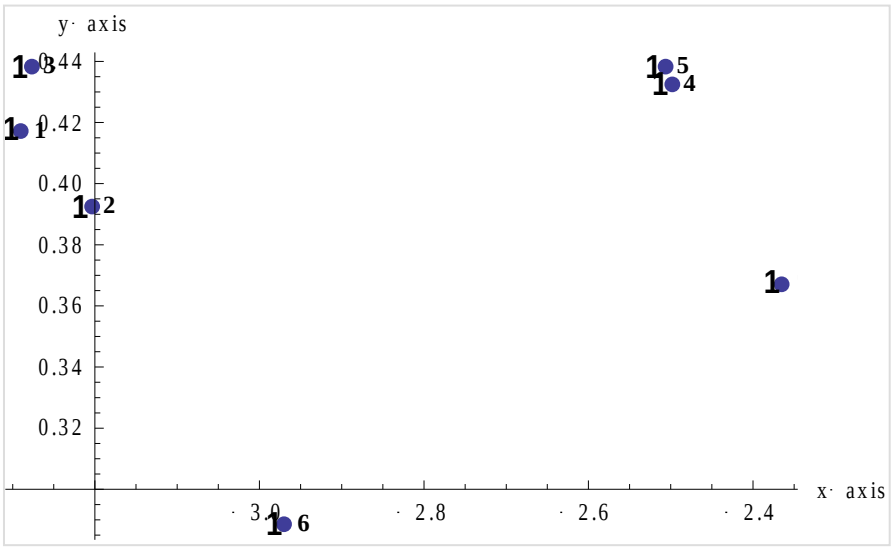

ЗМТА

```
{0.0400244,      80.7691,      80.7691},
{0.00612877,     12.3678,      93.137},
{0.00146547,     2.95732,      96.0943},
{0.000730291,    1.47372,      97.568},
{0.00046277,     0.933867,     98.5019},
{0.000249813,    0.504122,     99.006},
```

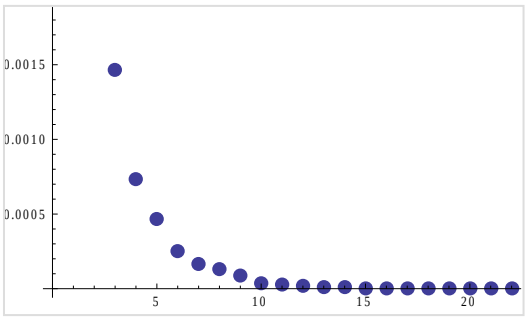

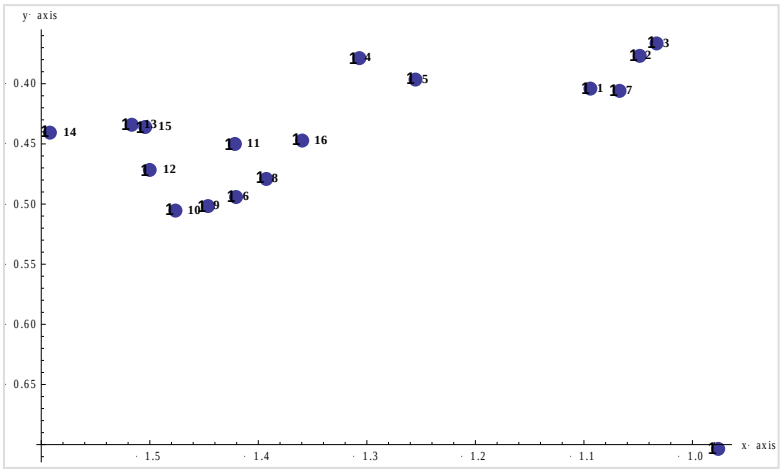

ЗМТА_с

```
{0.035504,        88.9628,          88.9628},
{0.00205245,      5.14283,          94.1056},
{0.00100312,      2.51353,          96.6191},
{0.000533027,     1.33561,          97.9547},
{0.000276111,     0.691854,         98.6466},
{0.000174913,     0.43828,          99.0849},
```

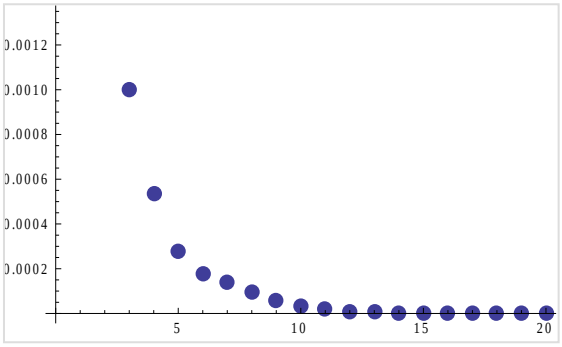

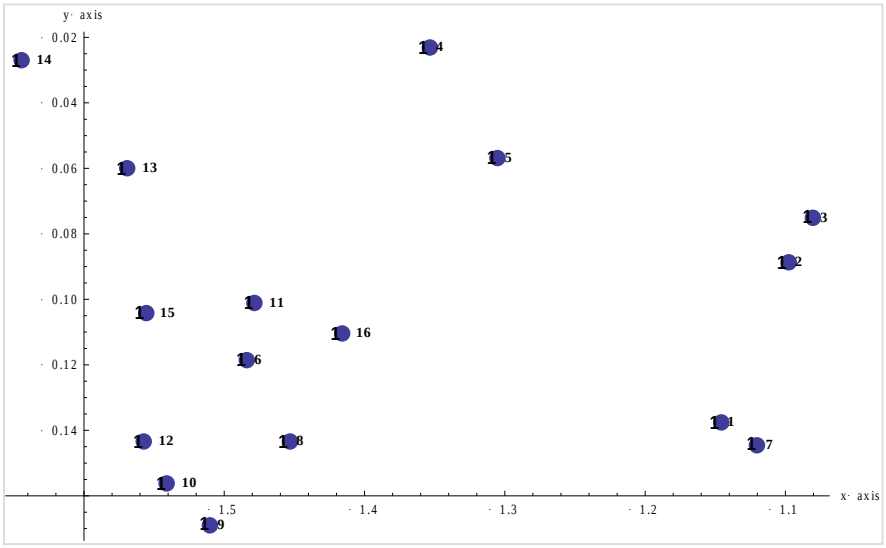

ЗМТВ

```
{0.0545264,        94.5657,          94.5657},
{0.00105578,       1.83105,          96.3967},
{0.000748574,      1.29826,          97.695},
{0.000594274,      1.03065,          98.7256},
{0.000313427,      0.543579,         99.2692},
{0.000177487,      0.307817,         99.577},
```

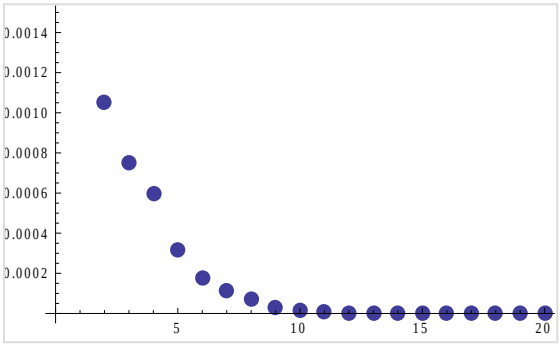

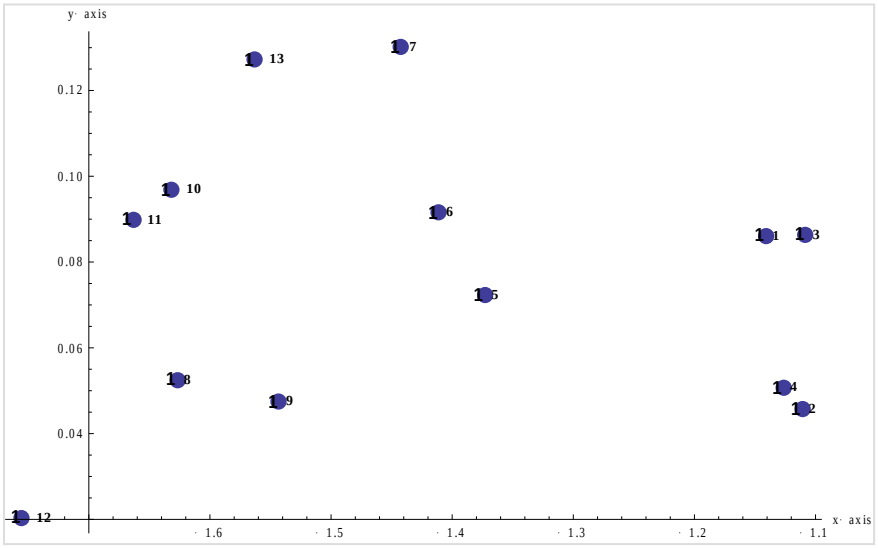

ЗМТС

```
{0.0576161,          93.1831,          93.1831},
 {0.0021513,         3.47932,          96.6624},
 {0.000625549,       1.01171,          97.6742},
 {0.000441489,       0.714023,         98.3882},
 {0.000373844,       0.604621,         98.9928},
 {0.000251929,       0.407446,         99.4002},
```

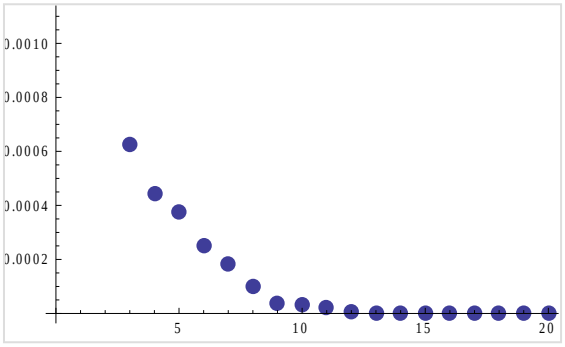

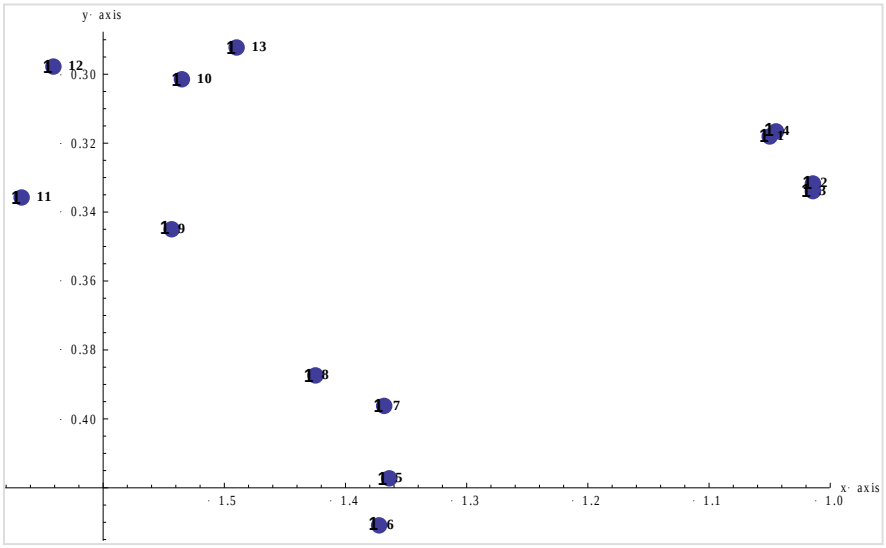

3MTD

```
{0.0244024,       94.5523,          94.5523},
{0.000750422,     2.90767,          97.4599},
{0.000280308,     1.08611,          98.546},
{0.000192743,     0.746823,         99.2929},
{0.000086909,     0.336747,         99.6296},
{0.0000599107,    0.232137,         99.8617},
```

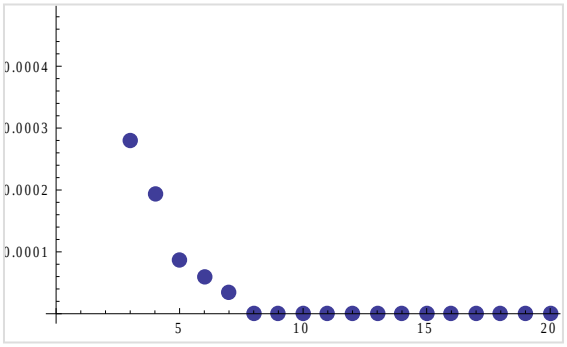

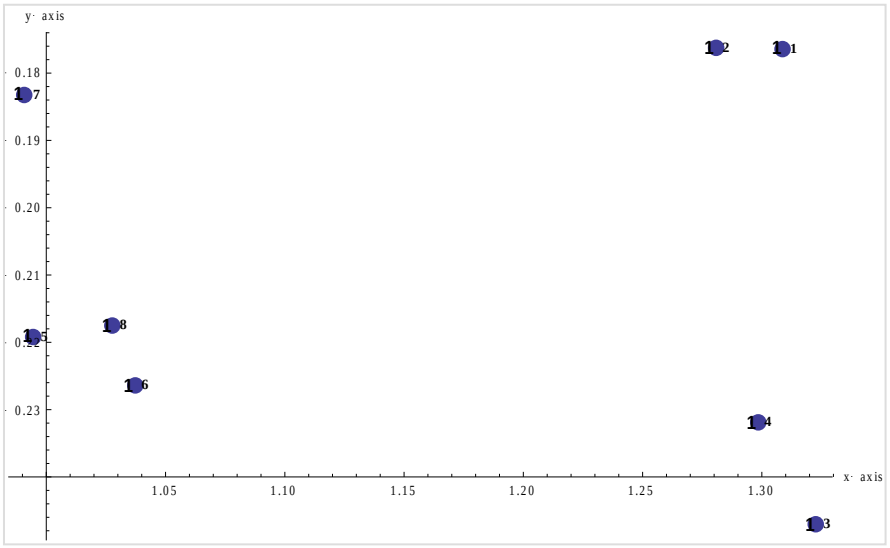

NASA

```
{0.066595,        93.9093,          93.9093},
{0.00196965,      2.77752,          96.6868},
{0.00079945,      1.12735,          97.8141},
{0.000761977,     1.07451,          98.8886},
{0.000294603,     0.415436,         99.3041},
{0.000192646,     0.271661,         99.5757},
```

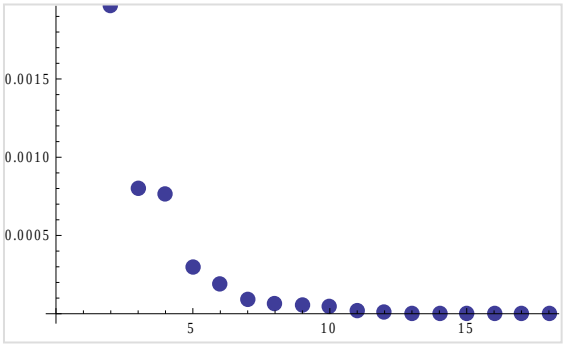

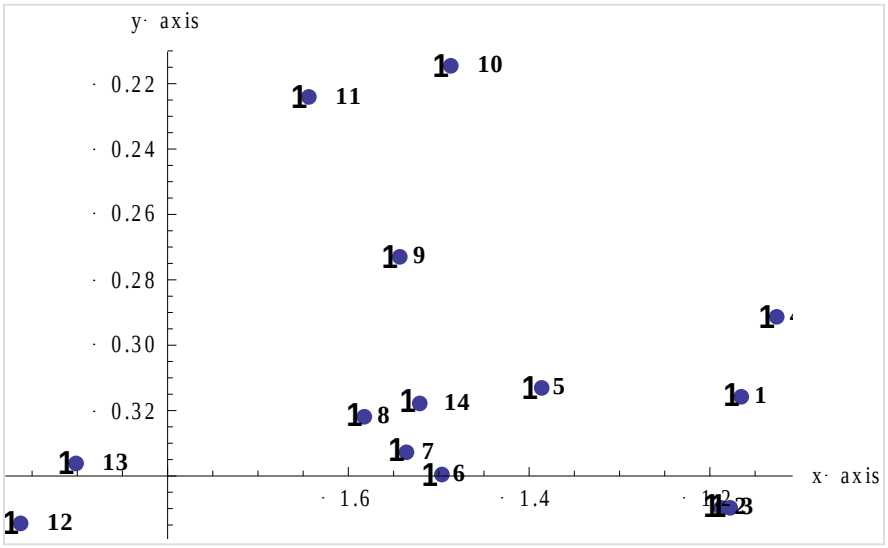

NASB

```
{0.059066,      92.322,      92.322},
{0.00215345,    3.3659,      95.6879},
{0.00103149,    1.61225,     97.3001},
{0.000466539,   0.729216,    98.0293},
{0.000410501,   0.641625,    98.671},
{0.000343333,   0.53664,     99.2076},
```

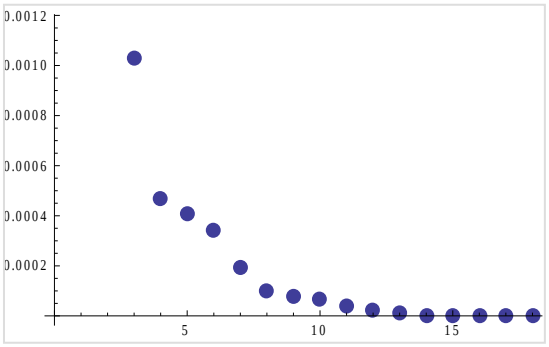

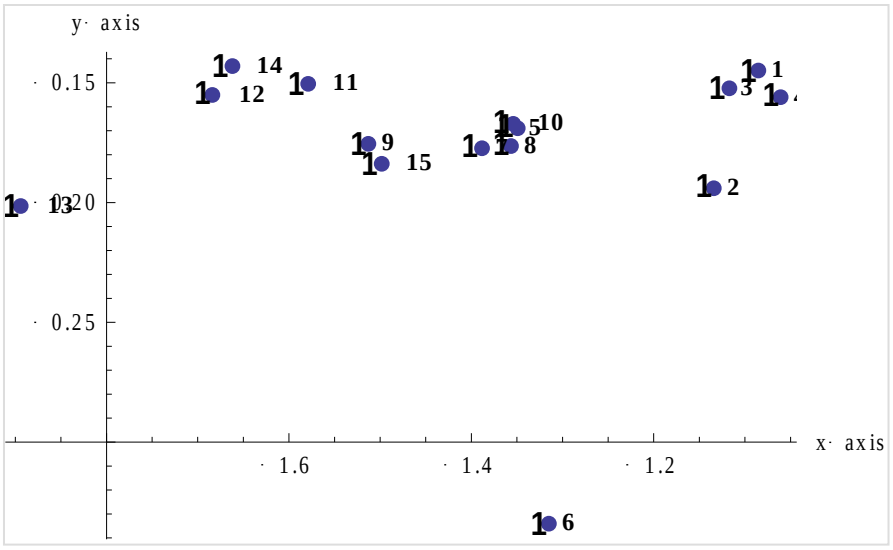

NASB_c

```
{0.0630278,      95.2136,          95.2136},
{0.00123428,     1.86458,          97.0781},
{0.000507209,    0.766221,         97.8444},
{0.000445331,    0.672743,         98.5171},
{0.000374857,    0.566282,         99.0834},
{0.000209301,    0.316182,         99.3996},
```

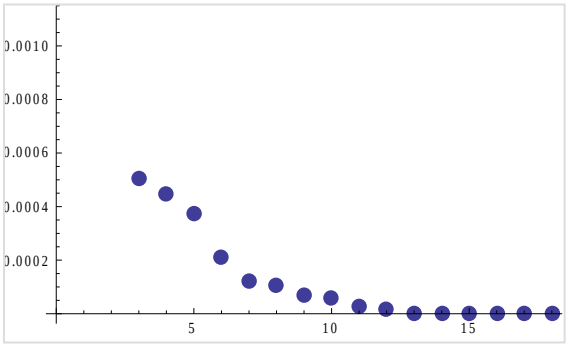

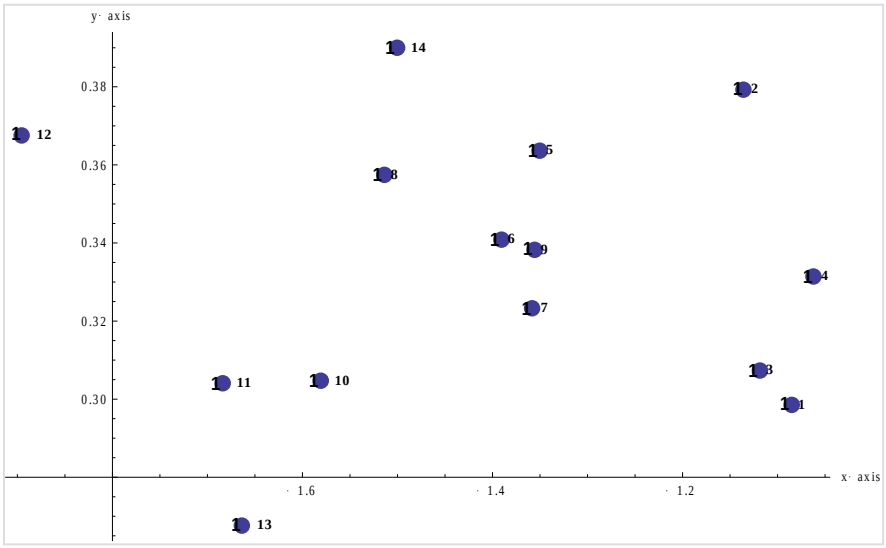

NASC

```
{0.0781904,      93.995,          93.995},
{0.00229101,     2.75409,         96.7491},
{0.00116968,     1.40611,         98.1552},
{0.000786855,    0.945903,        99.1011},
{0.000228571,    0.274772,        99.3759},
{0.000193139,    0.232178,        99.6081},
```

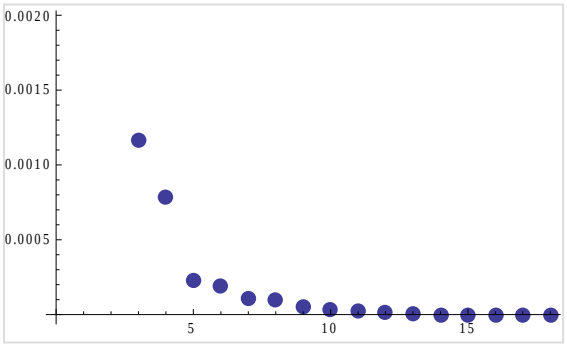

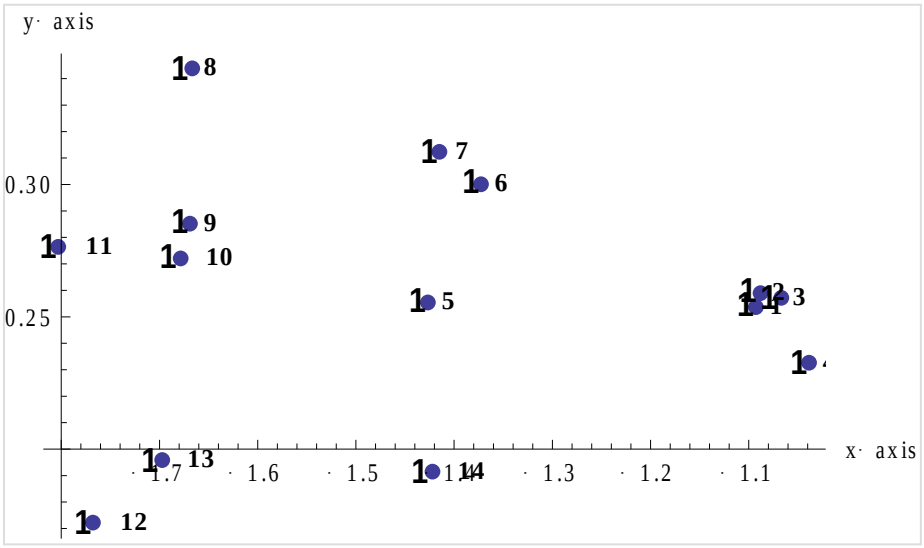

NASD

```
{0.108896,        92.8732,          92.8732},
{0.00465555,      3.97053,          96.8437},
{0.00244533,      2.08553,          98.9292},
{0.000700885,     0.597756,         99.527},
{0.000311374,     0.265559,         99.7925},
{0.000165266,     0.140948,         99.9335},
```

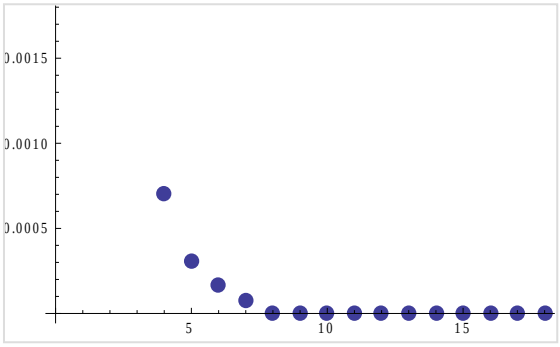

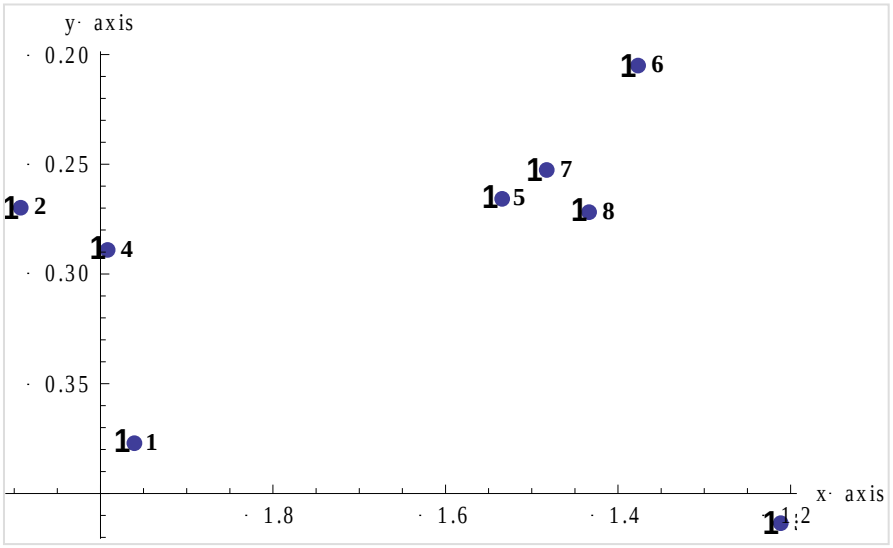

Appendix C Peaks used for Quantitative Comparisons

3M, 3MT, NAS Comparisons:

	12 roll comparison: 3M, 3MT, NAS	3M A,B,C,D	3MT A,B,C,D	NAS A,B,C,D	PE
	d(Å)	d(Å)	d(Å)	d(Å)	d(Å)
1	4.182	4.128	4.114	4.131	4.130
2	3.888	3.844	3.719	3.843	3.844
3	3.055	3.028	3.028	3.511	3.028
4	2.857	2.835	2.835	3.028	2.485
5	2.500	2.485	2.486	2.893	1.908
6	2.101	2.089	2.280	2.836	1.600
7	1.933	1.923	2.090	2.484	1.418
8	1.917	1.908	1.923	2.280	
9	1.880	1.871	1.908	2.089	
10	1.606	1.622	1.871	1.922	
11	1.520	1.600	1.601	1.908	
12	1.423	1.521	1.520	1.871	
13	1.340	1.508	1.515	1.622	
14	1.298	1.437	1.506	1.601	
15		1.418	1.437	1.521	
16		1.336	1.419	1.478	
17		1.294	1.354	1.419	
18		1.152	1.336	1.337	
19			1.295	1.295	
20			1.152		
21			1.059		

Blind Validation Study:

	A,E,I	C,H,N,Q,R	F,K,O,P	G,L,M	C,R,J	H,N,Q
	d(Å)	d(Å)	d(Å)	d(Å)	d(Å)	d(Å)
1	4.120	4.116	4.133	7.099	4.115	4.129
2	3.842	3.745	3.847	4.120	3.735	3.760
3	3.731	3.506	3.242	3.739	3.504	3.510
4	3.025	3.024	3.108	3.565	3.023	3.026
5	2.481	2.826	3.027	3.239	2.828	2.878
6	2.278	2.278	2.808	2.479	2.474	2.833
7	2.089	2.089	2.598	2.378	2.277	2.483
8	1.923	1.922	2.474	2.335	2.088	2.279
9	1.907	1.907	2.280	2.292	1.923	2.090
10	1.871	1.871	2.184	2.183	1.907	1.923
11	1.622	1.601	2.090	1.988	1.870	1.908
12	1.600	1.521	1.923	1.785	1.600	1.872
13	1.520	1.504	1.872	1.685	1.520	1.601
14	1.515	1.437	1.686	1.663	1.507	1.521
15	1.506	1.419	1.623	1.621	1.477	1.508
16	1.469	1.336	1.601	1.487	1.437	1.438
17	1.437	1.294	1.521	1.429	1.418	1.419
18	1.418		1.516	1.338	1.355	1.337
19	1.336		1.508	1.305	1.336	1.295
20	1.294		1.475	1.282	1.294	
21			1.438			
22			1.419			
23			1.377			
24			1.357			
25			1.336			
26			1.295			

VII. Cited References

M.J. Bradley et al, *Validation Study for Duct Tape End Matches*, Journal of Forensic Science, Volume 51, Issue 3, May 2006

Dr. S. Becker, *Trace evidence: A European perspective* , Trace Evidence Symposium, August 2007

J.F. Carter, *Forensic isotope ratio mass spectrometry of packaging tapes*, Analyst, 2004, 129, 1206–1210

V. Causin, A quantitative differentiation method for plastic bags by wide angle X-ray diffraction for tracing the source of illegal drugs, Forensic Science International 168 (2007) 37–41,

V. Causin et al. *Forensic differentiation of paper by X-ray diffraction and infrared spectroscopy*, Forensic Science International, Volume 197, Issues 1-3, 15 April 2010

R. Cook, I.W. Evett et al. *A hierarchy of propositions: deciding which level to address in casework*, Science & Justice 1998; 38(4): 231-239

M . Hida, *Classification of counterfeit coins using multivariate analysis with X-ray diffraction and X-ray fluorescence methods*, Forensic Science International , Volume 115, Issue 1 - 2 , Pages 129 - 134

A.Hobbs et al. *A New Approach for the Analysis of Duct Tape Backings*, Forensic Science Communications; January 2007 Vol 9 Number 1;

Ingman & Rudin, *The Origin of Evidence*, Forensic Science International 2002, 126, 11-16*:*

Author info not provided, *Forensic Examination of Soil Evidence*, 13th Interpol Forensic Science symposium, Lyon, France Oct 2001

J. Johnston, J.Serra. *The examination of pressure sensitive adhesive tapes*, IAMA Newsletter *(2005) 5(1):19–31.*

M. Kotrlý, *Application of X-ray diffraction in Forensic Science*, Z. Kristallogr. Suppl. 23 (2006) 35-40

P.C. Lowe, *Discrimination of Duct Tape Samples Using FTIR, SEM/EDS, and XRD Analysis*, Proceedings of the American Academy of Forensic Sciences February 2004, Orlando

S. Montero, W. Wiarda, P. de Joode, G. van der Peijl, *LA-ICP-MS and IRMS investigations on packaging and duct tapes*, FIRMS2005, March 2005.

C. Palenik, J. Buscaglia *Applications of Cathodoluminescence in Forensic Science*, in Forensic Analysis on the Cutting Edge edited by Robert Blackledge (2007)

C. Palenik, *Cathodoluminescence Microscopy in Forensic Science*, AAFS Annual Meeting Seattle 2006

D. F. Rendle, *X-Ray Diffraction in Forensic Science*, The Rigaku Journal, Vol 19 No 2 & Vol 20 No 1, 2003